Top Heterocycl Chem (2021) 58: 467–518
https://doi.org/10.1007/7081_2020_40

Published online: 10 October 2020

The Callipeltoside Story

James R. Frost and Steven V. Ley

Contents

Abstract In their search for novel molecules of therapeutic benefit during the 1990s, Minale and his team collected extracts from the shallow water lithistid marine sponge *Callipelta* sp. Subsequent testing of these specimens revealed promising activity in cytotoxic assays by inhibiting in vitro proliferation of KB and P388 cells. Whilst a closer inspection of the extract revealed callipeltins A–C as the major metabolites responsible for the observed activity, further analysis led to the discovery of three additional cytotoxic components: callipeltosides A, B and C (each differing in the attached sugar). At the time, these molecules represented a structurally unprecedented class of polyketides, rightly drawing the attention of the synthetic

J. R. Frost (✉)
UCB Pharma, Slough, UK
e-mail: james.frost@ucb.com

S. V. Ley (✉)
Department of Chemistry, University of Cambridge, Cambridge, UK
e-mail: svl1000@cam.ac.uk

community. Although the connectivity of these molecules could be deduced by Minale, questions surrounding the absolute stereochemistry of the sugar moieties (C1'–C8', D or L) and configuration of the *trans*-configured chlorocyclopropane with respect to the C1–C19 unit remained. Furthermore, the stereochemistry of the glycosidic linkage could not be conclusively determined. This chapter details the substantial effort of the synthetic community to elucidate the structure of these fascinating molecules from start to finish, describing nigh on 20 years of collective work by world leaders in the field.

Graphical Abstract

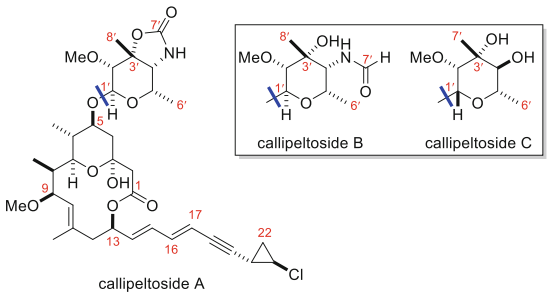

Keywords Aglycon · Callipeltoside · Carbohydrate · Chlorocyclopropane · Macrocycle

1 Isolation

Extracts from marine sponges have provided a large number of complex molecules that exhibit a wide range of biological activities. In their search for novel compounds that display antitumour and antiviral properties, Minale and his team examined an extract from the shallow water lithistid marine sponge *Callipelta* sp., located off New Caledonia [1, 2]. This specimen was found to inhibit the in vitro proliferation of P388 and KB cells whilst also providing protection against HIV. Further study of the extract indicated that callipeltins A–C were the major metabolites responsible for the biological activity [1, 2]. However, additional analysis of the dichloromethane extract of this marine sponge (2.5 kg freeze dried) revealed callipeltoside A as a minor metabolite (3.5 mg isolated) [3] and later callipeltosides B and C (both $\leq$1.0 mg) (Fig. 1) [4]. At the time of isolation, these polyketides represented an unprecedented new class of natural products, which has now been expanded upon with the disclosure of the phorbasides, aurisides, dolastatins and others [5, 6].

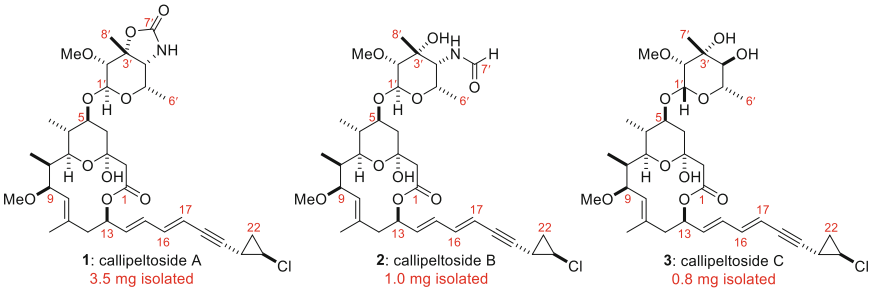

Fig. 1 The callipeltosides in their corrected forms

1.1 Structural Features and Assignment

1.1.1 Callipeltoside A

Minale and co-workers successfully deduced the connectivity of callipeltoside A through the use of COSY, HMQC and HMBC experiments. Further ROESY and nOe techniques provided an indication of the relative stereochemistry of the C1–C13 core whilst revealing the preferred chair conformation of the embedded C3–C7 pyran. Measurement of the ^{1}H coupling constant between C20 and C21 ($J_{20,21} = 3.1$ Hz, having removed additional $J_{21,22}$ splitting) gave strong evidence for a *trans*-configured chlorocyclopropane moiety. However, the configuration of the chlorocyclopropane with respect to the rest of the molecule could not be determined [3].

The attached 4-amino-4,6-dideoxy-2-*O*,3-*C*-dimethyl-α-talopyranosyl-3,4-urethane (later named callipeltose A) sugar was also without precedent. HMBC correlations between C5 and H1′ as well as H5 and C1′ provided the point of attachment for the glycosidic linkage, with nOe experiments giving evidence for the relative stereochemistry, suggesting an α-anomeric linkage. The nOe correlations also indicated that the pyran ring adopted a six-membered boat conformation, which was imparted by the five-membered cyclic carbamate [3].

Although the connectivity of callipeltoside A had been established, the absolute configuration could not be determined, and therefore the power of total synthesis was required to confirm the structure [3]. It was later shown by Trost [7, 8] (and also Evans [9, 10], Paterson [11], Panek [12], Hoye [13] and Ley [14, 15] vide infra) that the C1–C19 fragment and callipeltose A sugar were enantiomeric to that originally reported by Minale, whilst the chlorocyclopropane (C20–C22) was incorrectly configured with respect to the rest of the molecule (Fig. 2).

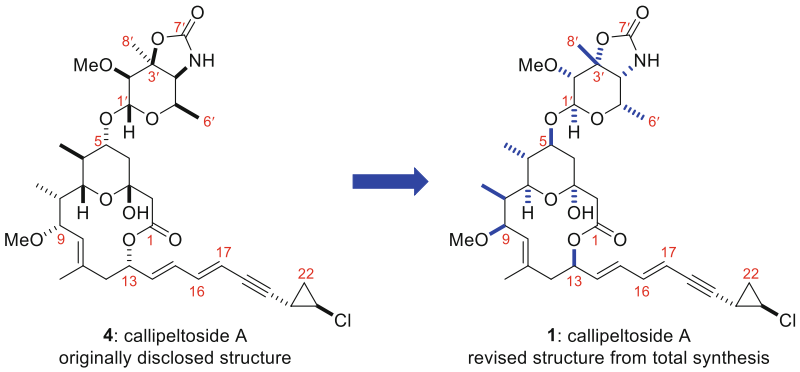

Fig. 2 Originally disclosed structure of callipeltoside A and subsequent absolute assignment following total synthesis

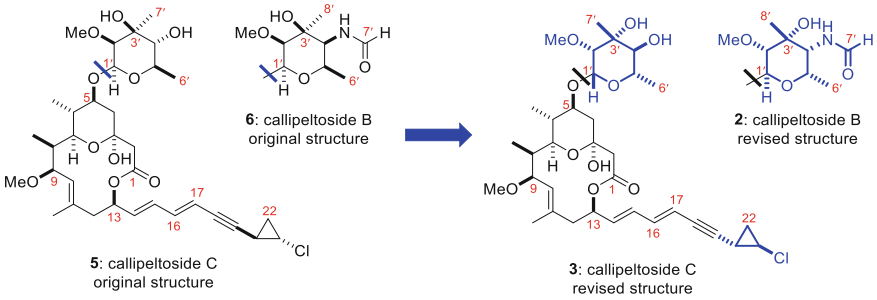

Fig. 3 Originally disclosed structures of callipeltosides B and C and subsequent absolute stereochemical assignment following total synthesis

1.1.2 Callipeltosides B and C

The structures of callipeltosides B and C were assigned in much the same way as callipeltoside A, with the authors suggesting them to contain 'the same macrolide portion including stereochemistry' as the parent molecule, the only difference being the attached sugar. Despite this comment, the isolation paper unusually depicts the structures of callipeltosides B and C as having an enantiomeric C1–C13 core to callipeltoside A (Fig. 3), also showing an oppositely configured chlorocyclopropane. Although Minale made no claim to know the absolute stereochemistry of callipeltosides A, B or C, the relative configuration described in the text and accompanying structures differed in their descriptions [4].

In keeping with the originally depicted structure of callipeltoside A, callipeltosides B and C were also shown to contain D-configured sugars. The configuration of these sugars was assigned on the basis that callipeltose C bore a likeness with the evalose sugar in everninomicin B [4].

The callipeltose B sugar was identified to contain an *N*-formyl group at the C4′H position, meaning that the molecule existed as 'two inseparable conformers' in a 4:1 ratio, whilst callipeltose C instead contained a secondary hydroxy group with opposite stereochemistry. Both the callipeltose B and C sugars were found to adopt chair conformations (following nOe experiments), with analysis of the ^{13}C NMR chemical shifts (extrapolated from HMQC experiments) indicating that the anomeric linkage was β-equatorial in both cases (callipeltoside B, $\delta = 99.2$; and callipeltoside C, 98.9 ppm) [4].

The first synthesis of callipeltoside C was completed by MacMillan in 2008 (Sect. 2.8), confirming that the absolute stereochemistry of the molecule in terms of the C1–C13 core, chlorocyclopropane unit and sugar configuration (L-configured rather than the original D-configuration suggested by Minale) were identical to callipeltoside A (Fig. 3). The configuration of the glycosidic linkage was tentatively suggested to be β-equatorial 'based on the isolation studies for callipeltoside B' [16].

The Ley group completed the synthesis of callipeltoside C in 2012 [14, 15], confirming the structural assignment by MacMillan [16]. Measurement of the $^{1}J_{C-H}$ coupling value of the glycosidic bond and thorough NOESY analysis of the sugar portion implied that the stereochemistry at C1′H was (*R*)-configured, in contrast to callipeltoside A. In the same work, this group also disclosed the first total synthesis of callipeltoside B, noting that the callipeltose B sugar was also L-configured, but with (*S*)-stereochemistry at the C1′H position. No further studies were performed, but it was reasonably assumed that the inversion of stereochemistry at the C1′H position for callipeltoside C is connected to the opposing configuration of the C4′H substituent (Fig. 3) [14, 15].

1.2 Biological Activity of the Callipeltosides

1.2.1 Studies by Minale

Preliminary studies by Minale indicated that callipeltoside A was moderately cytotoxic in assays against human bronchopulmonary non-small-cell lung carcinoma, affecting the NSCLC-N6 and P388 cell lines ($IC_{50} = 11.26$ and 15.26 μg/mL, respectively) [3]. Further research involving the NSCLC-N6 cell line showed a cell cycle-dependent effect, with cell division blocked at the G1 phase level (Table 1). However, the small amounts of isolated material prevented additional investigation into this process and hence determination of the exact mode of action [3].

Callipeltosides B and C also showed cytotoxic activity against the NSCLC-N6 cell line, albeit at a more modest level (IC_{50} values of 15.1 μg/mL and 30.0 μg/mL, respectively) [4].

Table 1 Flow cytometry assays of the NSCLC-N6 cell line treated with callipeltoside A

	Concentration (μg/mL)	Cells in the G1 phase (%)	Cells in the S phase (%)	Cells in G2/M phase (%)
Control		67.9	28.0	4.1
Callipeltoside A (1)	30	82.5	14.9	2.6
	10	77.5	20.8	1.7
	5	74.7	22.6	2.7

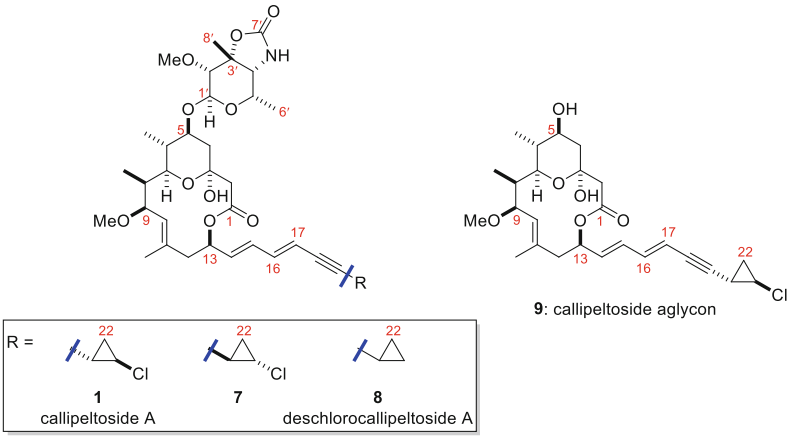

Fig. 4 Compounds synthesised and tested by Trost against the A2780 human ovarian carcinoma cell line

Table 2 Assays against the A2780 human ovarian carcinoma cell line

Entry	Compound	IC_{50} (μM)
1	**1**	20.2
2	**7**	7.0
3	**8**	17.4
4	**9**	>100

1.2.2 Studies by Trost

Further investigations into the biological activity of callipeltoside A were carried out by Trost and co-workers [8]. During their synthesis of callipeltoside A, diastereomer **7**, deschlorocallipeltoside A (**8**) and the callipeltoside aglycon (**9**) were also synthesised (Fig. 4).

Treatment of A2780 human ovarian carcinoma cells (following 48 h incubation) with callipeltoside A as well as **7**, **8** and **9** showed that the callipeltose A sugar was essential for biological activity, whilst the *trans*-chlorocyclopropane was less critical (Table 2, entries 1 and 3). Interestingly the introduction of the oppositely configured *trans*-chlorocyclopropane (**7**) resulted in improved biological activity relative to the natural product (Table 2, entry 2) [8].

2 Structural Investigations and Total Syntheses

The first total synthesis of callipeltoside A (**1**) was completed in 2002 by Trost [7, 8], following excellent initial work by Paterson who completed what proved to be the enantiomeric C1–C13 core (2001) [17].

The synthesis of callipeltoside A was also achieved thereafter by the groups of Evans (2002) [9, 10], Paterson (2003) [11], Panek (2004) [12], Hoye (2010) [13] and Ley (2012) [14, 15]. In addition, a formal synthesis of the callipeltoside aglycon has been disclosed by Marshall [18], partial syntheses by Olivo [19–21] and Yadav [22] as well as numerous contributions towards the callipeltose A sugar [23–26]. The absolute configuration of callipeltoside C (**3**) was initially determined by MacMillan (2008) [16], whilst the Ley group supported this assignment and completed the family with the first synthesis of callipeltoside B [14, 15]. Due to the page restriction imposed on this review, only the completed syntheses of these molecules and subsequent learnings will be reported.

2.1 Paterson Aglycon Synthesis (2001)

2.1.1 Retrosynthesis

Paterson's approach to the callipeltoside aglycon involved disconnection along the C1–C13O ester linkage which, in the forward direction, would be formed by Yamaguchi macrolactonisation. Since the relative configuration of the *trans*-chlorocyclopropane with respect to the rest of the molecule was in doubt, attachment of each enantiomer was necessary. Therefore, the C17–C18 bond was chosen as a further key disconnection point, revealing vinyl iodide **11** and the cyclopropyl alkyne **12**. Compound **11** was further disconnected at the pyran moiety, giving fragment **13**, which in turn could be accessed through sequential aldol reactions. This strategy therefore allows the facile synthesis of both C13 epimers and allows for the relative configuration of the macrolide ring to be resolved (Scheme 1) [17].

2.1.2 Synthesis of the C1–C17 Vinyl Iodide

The synthesis began by union of known vinyl iodide **17** and the enolate of enal **16** by Lewis acid-mediated vinylogous aldol reaction [17, 27, 28]. This resulted in an intentional 1:1 mixture of epimeric products at C13, also installing the desired trisubstituted double bond present in the natural product scaffold [17]. TBS protection of the C13 alcohol followed by boron-mediated *anti*-aldol reaction with **15** set the C8 and C9 stereocentres [17, 29–31]. Diastereoselective reduction of the ketone functionality using the Evans–Tishchenko protocol formed the remaining C7

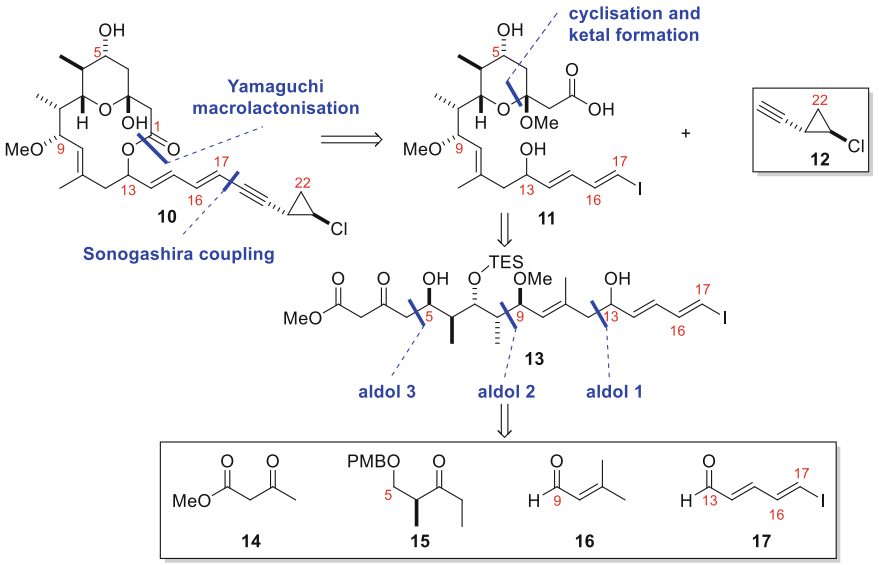

Scheme 1 Paterson's retrosynthesis of the callipeltoside aglycon

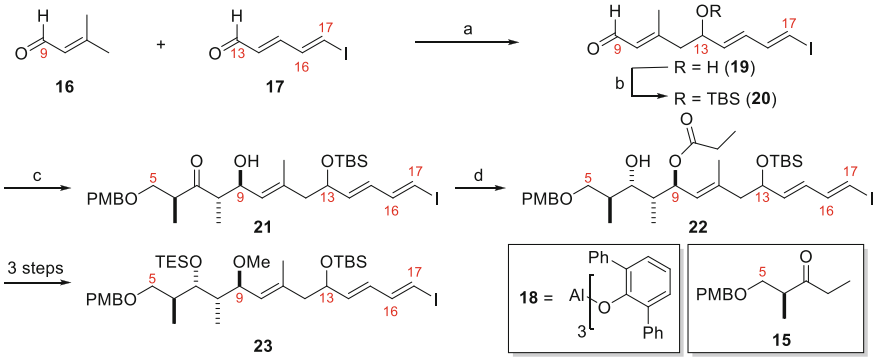

Scheme 2 Synthesis of C5–C17 fragment **23.** *Reagents and conditions*: (**a**) **16**, PhMe, −78°C; LDA, then **17**, **18**, THF, −78°C, 80%; (**b**) TBSCl, imidazole, CH_2Cl_2, RT, 87%; (**c**) (i) Cy_2BCl, Et_3N, Et_2O, −5°C, then **15**, −78°C to −27°C; (ii) CH_2Cl_2–H_2O, SiO_2, RT, 99% (over 2 steps), dr > 98.5:1.5; (**d**) SmI_2, EtCHO, THF, −20°C to −10°C, 92%, dr > 98.5:1.5

stereocentre in high selectivity. A further three synthetic manipulations provided advanced protected C5–C17 fragment **23** (Scheme 2) [17].

PMB protecting group removal and oxidation gave aldehyde **24**, which underwent Mukaiyama aldol reaction with **25** to give linear precursor **26** in good diastereoselectivity (95:5) and yield (85%). Acid-catalysed deprotection of the TES group resulted in cyclisation and methyl ketal formation to give **27** in an excellent yield of 96% (Scheme 3) [17].

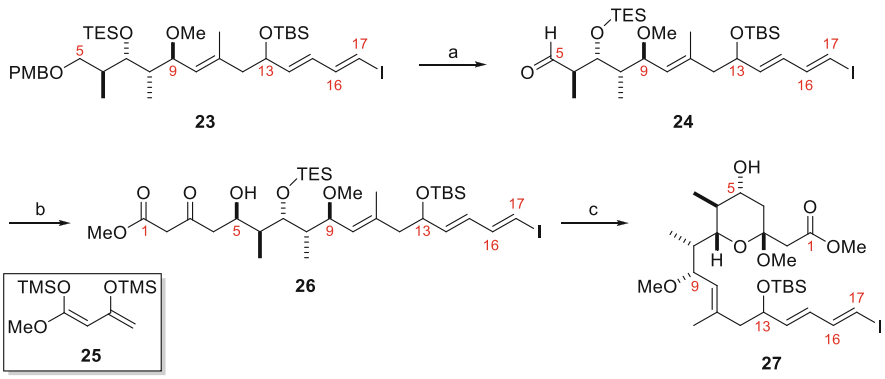

Scheme 3 Manipulation of the C1–C17 fragment and formation of the C3–C7 pyran. *Reagents and conditions*: (**a**) (i) DDQ, CH_2Cl_2–pH 7 buffer (10:1), 40°C, 88%; (ii) Dess–Martin periodinane, CH_2Cl_2, RT, 86%; (**b**) **25**, BF_3•OEt_2, CH_2Cl_2, −100°C, 85%, dr = 95:5; (**c**) PPTS, $(MeO)_3CH$, MeOH, 20°C, 96%

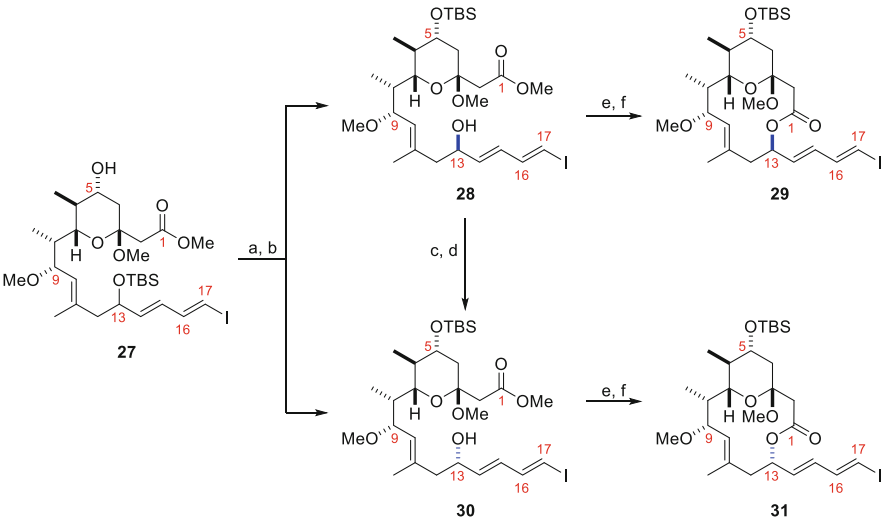

Scheme 4 Formation of the proposed callipeltoside macrocycle and the C13 epimeric material. *Reagents and conditions*: (**a**) TBSCl, imidazole, CH_2Cl_2, RT; (**b**) TBAF, THF, RT, 87% (over 2 steps); (**c**) TPAP, NMO, 4 Å MS, CH_2Cl_2, RT; (**d**) $NaBH_4$, $CeCl_3$•$7H_2O$, EtOH, −78°C to 0°C, 46% (over 2 steps); (**e**) $Ba(OH)_2$•$8H_2O$, MeOH, RT; (**f**) 2,4,6-trichlorobenzoyl chloride, Et_3N, DMAP, PhMe, 80°C, 53% (over 2 steps, **28** to **29**) and 70% (over 2 steps, **30** to **31**)

The free hydroxy was protected as the TBS-ether and the C13OH revealed thereafter following selective removal of the TBS group using TBAF. This allowed for separation of the C13 epimeric alcohols, which could then be separately saponified and the requisite 12-membered rings formed by Yamaguchi macrolactonisation (Scheme 4) [17]. With the two macrocycles in hand, the Paterson group used

molecular modelling and compared the nOe data collected by Minale [3]. The group concluded that macrocycle **31** was more likely the desired conformation, and so the unwanted isomer (**28**) was recycled by oxidation and diastereoselective reduction prior to saponification (Scheme 4) [17].

2.1.3 Synthesis of Enantiomeric *trans*-Chlorocyclopropyl Alkynes 12 and *ent*-12

The synthesis of enantiomeric *trans*-chlorocyclopropyl alkynes **12** and *ent*-**12** was achieved using an asymmetric Simmons–Smith cyclopropanation developed by the Charette group [32–34]. Following this, oxidation, dibromoolefination and Corey–Fuchs reaction gave the *trans*-chlorocyclopropane **12** in short sequence (Scheme 5, one enantiomer shown) [17].

2.1.4 Synthesis of Diastereomeric Aglycons 39 and 41

Cyclopropyl alkynes **12** and *ent*-**12** were cross-coupled with the C1–C17 vinyl iodide (**31**) by Sonogashira reaction to give **38** and **40**. Each molecule underwent TBS deprotection, with treatment using PPTS in H_2O installing the hemi-ketal functionality. The diastereomeric aglycons **39** and **41** were synthesised in 54% (over 3 steps) and 67% (over 3 steps), respectively (Scheme 6) [17].

The ^1H and ^{13}C NMR data for diastereomeric aglycons **39** and **41** were found to be near identical, preventing any conclusive assignment. However, the *trans*-chlorocyclopropane influenced the optical rotation of these molecules, which was found to be significantly different in both sign and magnitude [**39**, $[\alpha]_D^{20} = -97.8$ ($c = 0.19$, $CHCl_3$); **41**, $[\alpha]_D^{20} = +45.8$ ($c = 0.28$, $CHCl_3$)] [17]. This result outlined the importance of the optical rotation for the structural determination of

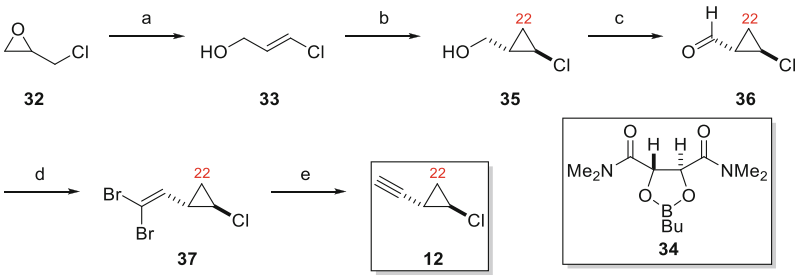

Scheme 5 Access to enantiomeric cyclopropyl alkynes (one enantiomer shown; **12**). *Reagents and conditions*: (**a**) *n*-BuLi, TMEDA, THF, −78°C to 0°C, 80%; (**b**) $ZnEt_2$, CH_2I_2, **34**, CH_2Cl_2, 0°C to RT, dr = 97.5:2.5; (**c**) $(COCl)_2$, DMSO, CH_2Cl_2, −78°C, then Et_3N, −78°C to 0°C; (**d**) Zn, pyridine, PPh_3, CBr_4, CH_2Cl_2, RT, 40% (over 3 steps); (e) *n*-BuLi, Et_2O, −78°C, no reported yield, used directly in the next step

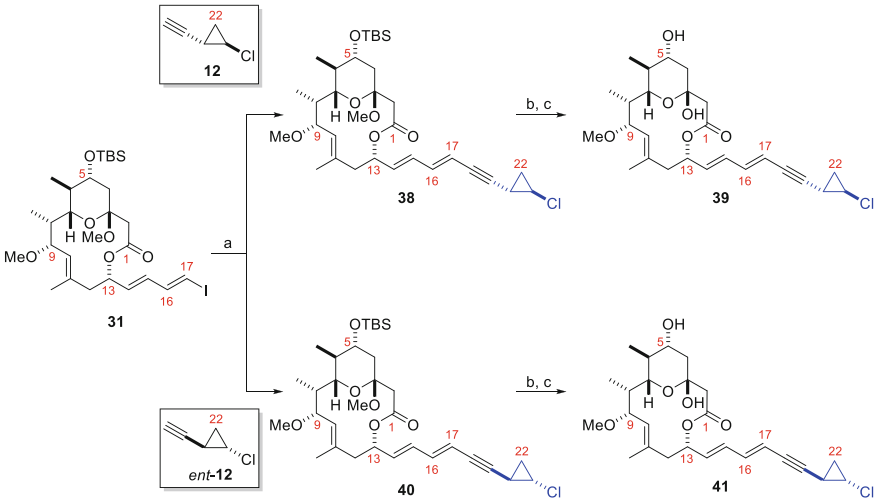

Scheme 6 Synthesis of diastereomeric aglycons **39** and **41.** *Reagents and conditions*: (**a**) **12** or *ent*-**12** [$(PPh_3)_2PdCl_2$], CuI, *i*-Pr_2NH, EtOAc, −20°C to RT; (**b**) TBAF, THF, RT; (**c**) PPTS, MeCN, H_2O, RT, 54% (over 3 steps, **31** to **39**), and 67% (over 3 steps, **31** to **41**)

callipeltoside A. However, at this point in time, attachment of the callipeltose A sugar was not reported by Paterson, and therefore the absolute configuration of callipeltoside A was not determined.

2.2 Trost Synthesis of Deschlorocallipeltoside A (8)

Prior to their synthesis of callipeltoside A, the Trost group completed deschlorocallipeltoside A (**8**) [35]. By targeting **8**, Trost hoped to confirm the relative stereochemistry of the C1–C22 core with respect to the callipeltose A sugar and provide a convergent strategy to this family of molecules [8, 35]. Comparison of callipeltoside A with auriside B (**42**) revealed several structural similarities (Fig. 5), suggesting that the synthetic effort should focus on the synthesis of the enantiomeric C1–C13 portion (to that disclosed by Paterson) and an L-configured sugar [8, 35, 36].

2.2.1 Retrosynthesis

Initial retrosynthetic disconnections involved the late-stage attachment of the callipeltose A sugar (**43**) by Schmidt glycosidation and Horner–Wadsworth–Emmons (HWE) coupling of the C1–C13 macrocycle with phosphonate **45** [8, 35]. Attachment of these fragments at a late stage meant that the stereochemical

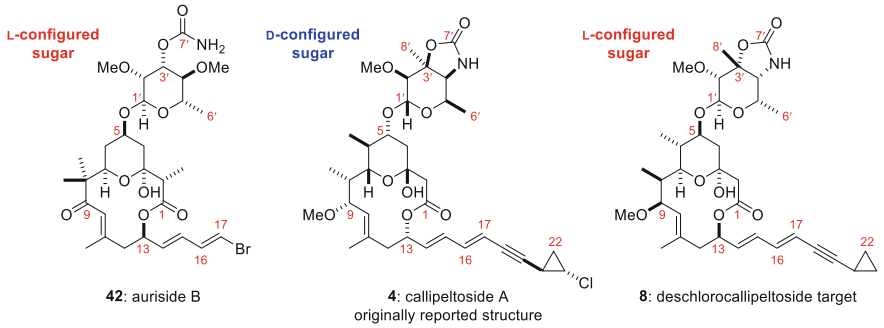

Fig. 5 Comparison of the callipeltoside scaffold with auriside B (**42**)

uncertainties associated with callipeltose A and the *trans*-chlorocyclopropane unit (for the synthesis of callipeltoside A) could be resolved at the end of the synthesis. Callipeltose A **43** was to be constructed from L-rhamnose (**46**), with phosphonate **45** by Sonogashira reaction between iodoalkyne **48** and cyclopropyl alkyne **49** followed by further synthetic manipulation [8, 35]. An acylketene cyclisation would provide the C1–C13 macrocycle, whilst a ruthenium-Alder-ene type coupling [37] and palladium-catalysed allylic alkylation [38] would be key to the synthesis of substrate **47** (Scheme 7) [8, 35].

2.2.2 Synthesis of the C1–C13 Macrocycle 44

Synthesis of the C1–C13 macrocycle began from (*S*)-configured Roche ester **50**, which was converted into alkyne **51** in 5 linear steps [8, 35]. A ruthenium-catalysed Alder-ene type reaction between **51** and **52** was implemented to construct **53**, with the trisubstituted double bond formed with complete regioselectivity (Scheme 8) [8, 35, 37]. Incorporation of the Troc protecting group was key to obtaining high yield (85%), lower catalyst loading (5 mol%) and shorter reaction time (30 min) compared to the unprotected version (62%, 10 mol%, 2 h, respectively) [8, 35]. The regioselectivity of this reaction was thought to arise from ruthenium metallacycle **58** (Scheme 9), with a dative interaction between the non-bonding methoxy electrons and ruthenium essential to reduce the equilibration of the oxidative cyclisation and enhance the rate of the β-hydride elimination step [8, 37].

The C13 stereocentre was installed via an asymmetric palladium-catalysed allylic alkylation reaction with (*R*,*R*)-diphenyl compound **61** identified as the chiral ligand of choice, providing **55** in excellent diastereoselectivity (95:5), good yield (79%) and reasonable branched-to-linear ratio (75:25) [8, 35, 38]. The proposed mechanism for this transformation is shown in Scheme 10 [8, 38]. It is postulated that following alkene coordination to the active palladium species, the corresponding palladium π-allyl species forms with loss of the OTroc group and formation of the putative cationic complex **62** [8]. It is suggested that the *anti*-π-allyl species is favoured over

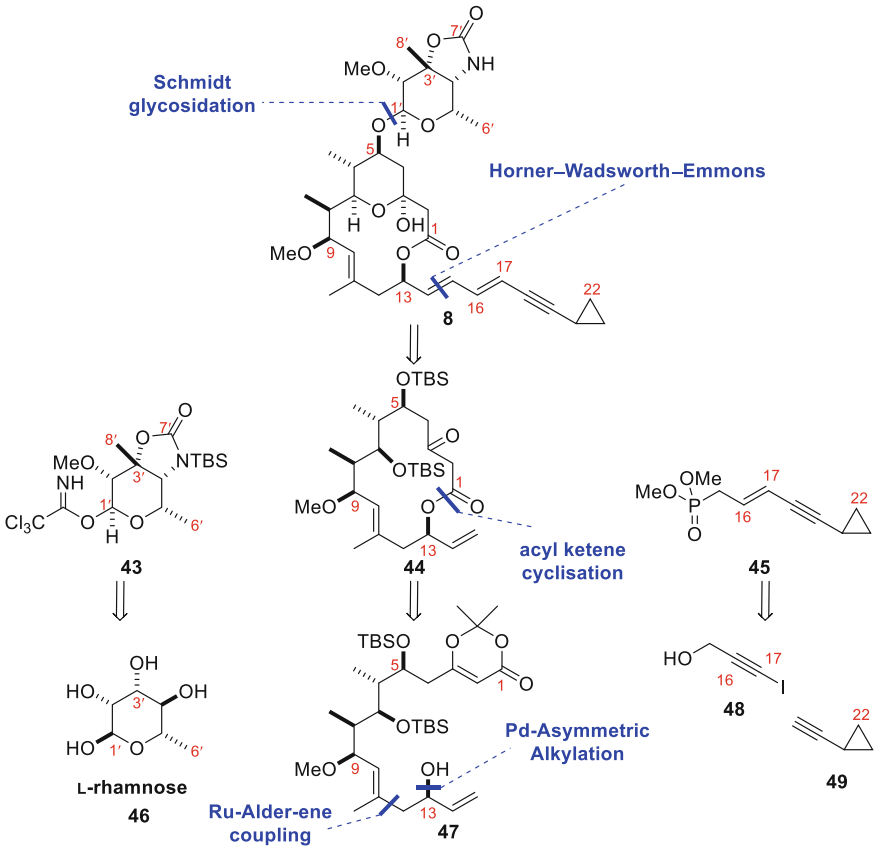

Scheme 7 Trost retrosynthesis of deschlorocallipeltoside A (**8**)

the *syn*-π-allyl form by virtue of the increased steric bulk of the substituted *syn*-π-allyl configuration [8]. The (*R*,*R*)-diphenyl ligand **61** is key for setting the C13 stereocentre, influencing the diastereofacial nucleophilic attack of *p*-methoxyphenol [8].

However, further analysis of C13 stereocentre using the *O*-methylmandelate method [39] revealed that the *undesired* C13 configuration had been set. Fortunately, this unanticipated result could be rectified by use of the enantiomeric (*S*,*S*)-diphenyl ligand **54** (see Scheme 8) in excellent diastereoselectivity (95:5) and slightly lower branched to linear regioselectivity (66:34) [8].

With the C13 stereocentre in place, routine deprotection and oxidation of the primary alcohol gave **69**. Addition of the *E*-lithium enolate of *t*-butylthiopropionate generated the C6 stereocentre in good diastereoselectivity (dr = 84:16) by means of a Cram chelation-controlled aldol reaction. Subsequent protection and reduction delivered aldehyde **70**, which was further reacted with **71** under Felkin–Anh control and protected as TBS-ether **72**. Treatment of **72** with CAN then liberated the C13

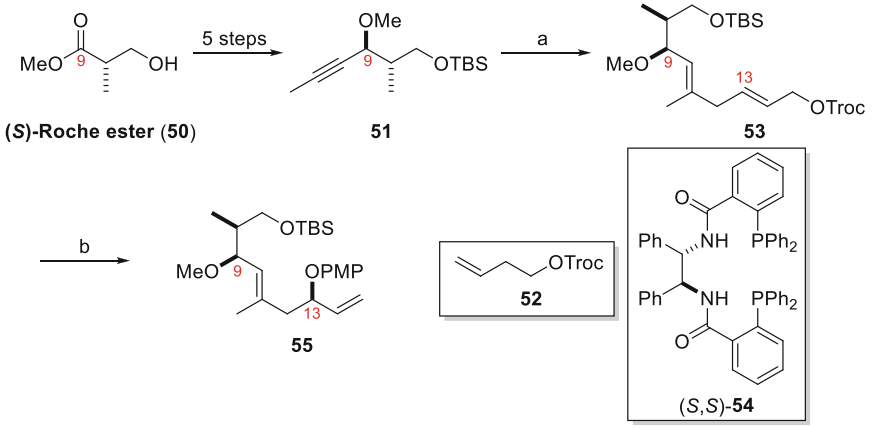

Scheme 8 Synthesis of C7–C15 fragment **55.** *Reagents and conditions*: (**a**) $CpRu(MeCN)_3PF_6$ (5 mol%), **52**, acetone, RT, 85%; (**b**) *p*-methoxyphenol, (*S*,*S*)-**54** (7.5 mol%), $[Pd_2dba_3]$•$CHCl_3$ (2.5 mol%), TBAC, CH_2Cl_2, 79%, dr = 95:5, regioselectivity = 66:34 (2°:1°)

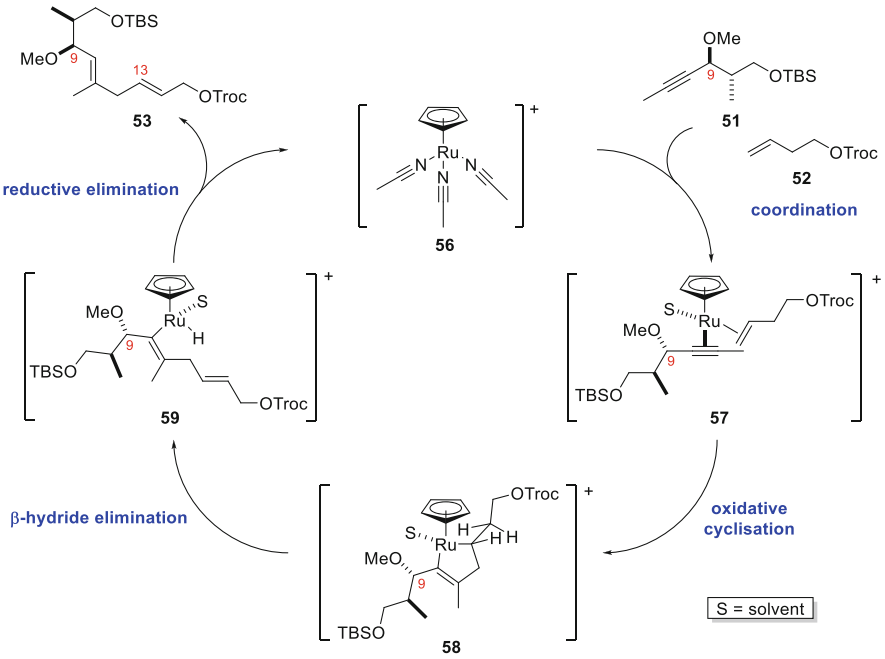

Scheme 9 Proposed mechanism for the ruthenium-catalysed Alder-ene reaction [8]

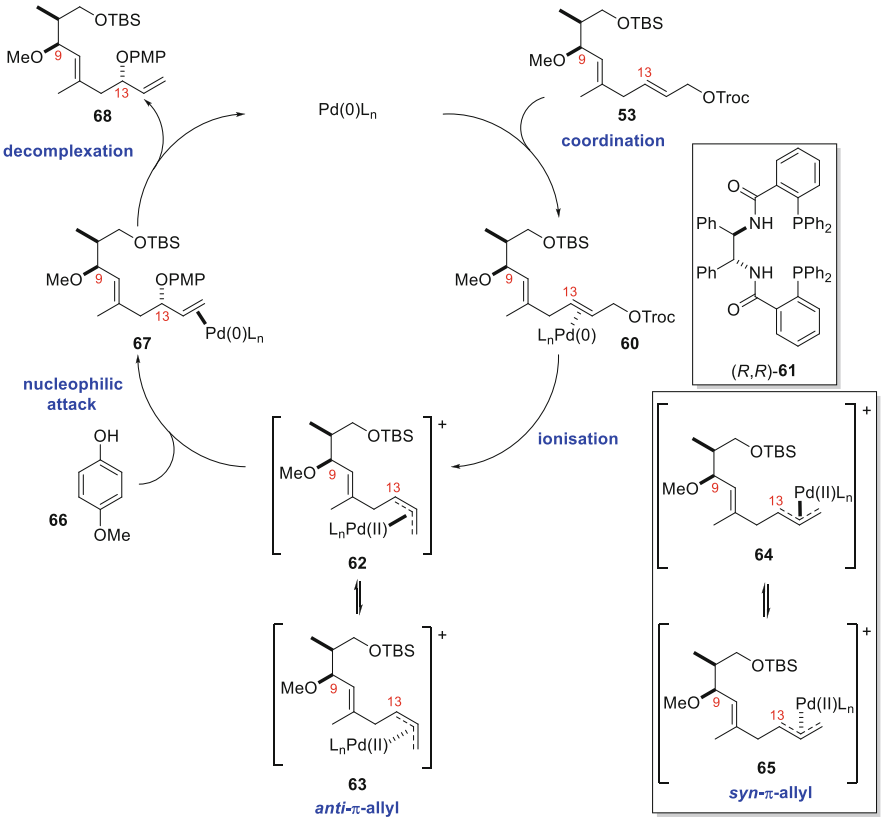

Scheme 10 Proposed catalytic cycle for the palladium-catalysed allylic alkylation using (*R*,*R*)-**61** [8]

alcohol which, upon heating, cyclised to produce the C1–C13 macrocycle (**44**) in 82% yield via the acyl ketene (Scheme 11) [8, 35].

2.2.3 Completion of the Deschlorocallipeltoside Aglycon 75

Dihydroxylation and sodium periodate-mediated cleavage converted macrocycle **44** to aldehyde **73**, with which the deschlorocallipeltoside sidechain **45**[1] could be appended via a Horner–Wadsworth–Emmons reaction [8, 35]. This was achievable in low yield (40%), with the *E*-isomer predominating in a 4:1 ratio. TBS deprotection

[1]This was synthesised by Sonogashira reaction between alkynyl iodide **48** and cyclopropyl alkyne **49** followed by stereoselective reduction, Appel reaction and displacement of the primary bromide with $P(OMe)_3$ [35].

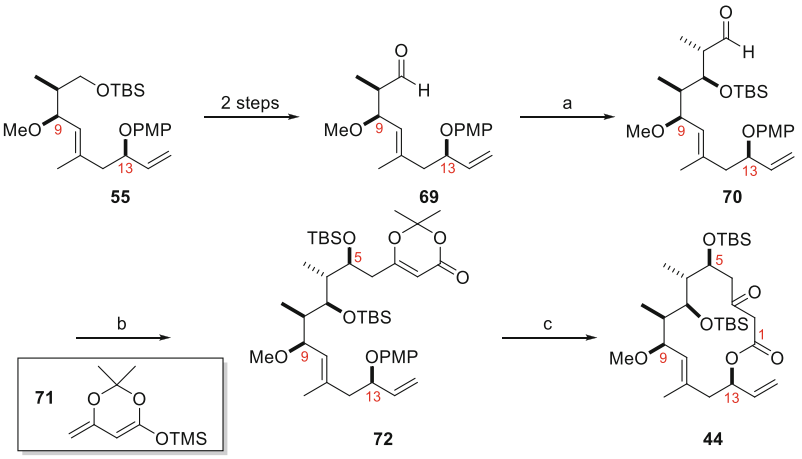

Scheme 11 Formation of macrocycle **44.** *Reagents and conditions:* (**a**) (i) *t*-butylthiopropionate, LDA, THF, −108°C, 82%, dr = 84:16; (ii) TBSOTf, 2,6-lutidine, CH_2Cl_2, 0°C, 86%; (iii) DIBAL-H, PhMe, −78°C, 79%; (**b**) (i) **71**, BF_3•OEt_2, CH_2Cl_2, −78°C, 94%, dr > 95:5; (ii) TBSOTf, 2,6-di-*t*-butylpyridine, CH_2Cl_2, 0°C, 95%; (**c**) (i) CAN, acetone–H_2O (4:1), 0°C, 82%; (ii) 0.5 mM in PhMe, 110°C, 82%

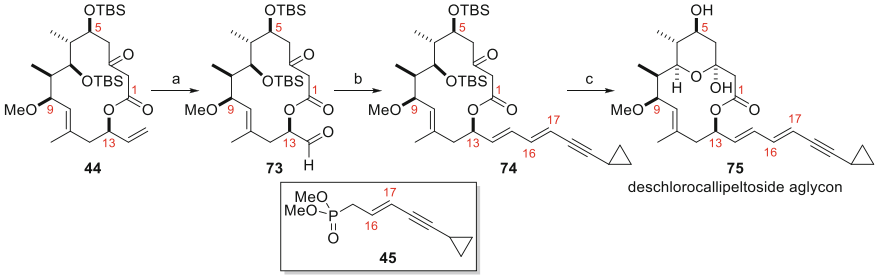

Scheme 12 Completion of the deschlorocallipeltoside aglycon **75.** *Reagents and conditions:* (**a**) OsO_4, NMO, THF–H_2O (4:1), 0°C, then $NaIO_4$, THF–H_2O, RT, 80%; (**b**) **45**, LiHMDS, THF, −78°C, 40%, *E*:*Z* = 4:1; (**c**) HF•pyridine, MeOH, RT, then PPTS, H_2O, MeCN, RT, 60%

and transketalisation with PPTS in wet MeCN then afforded the deschlorocallipeltoside aglycon **75** (Scheme 12) [35].

2.2.4 Synthesis of L-Callipeltose A (43) and Deschlorocallipeltoside A

The bicyclic ring system of callipeltose A (**76**) was synthesised according to previous methodology reported by Guiliano [25] starting from L-rhamnose. A three-step sequence then gave trichloroacetimidate **43**, in preparation for coupling

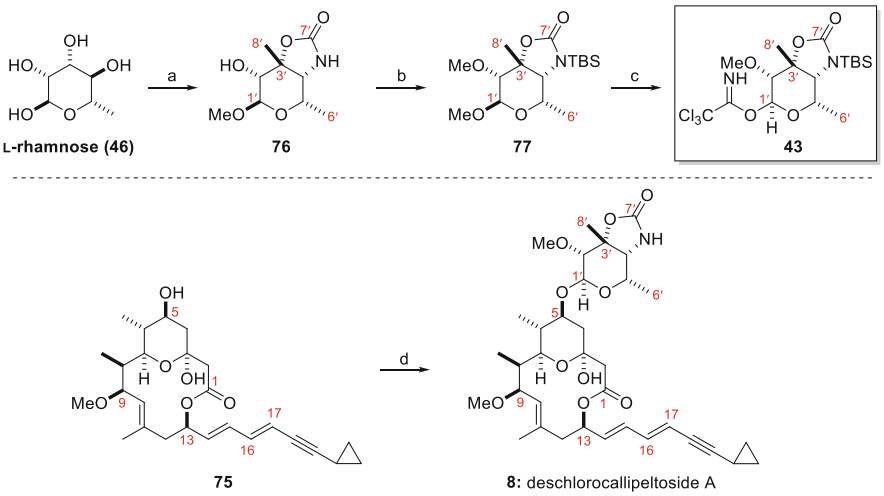

Scheme 13 Synthesis of callipeltose A (**43**) and deschlorocallipeltoside A (**8**). *Reagents and conditions*: (**a**) ref [25]; (**b**) (i) TBSOTf, 2,6-lutidine, CH_2Cl_2, RT, 55%; (ii) MeI, Ag_2O, DMF, RT, 69%; (**c**) (i) H_2SO_4, PPTS, Ac_2O, RT, 81%; (ii) K_2CO_3, MeOH, RT, 89%; (iii) Cl_3CCN, NaH, CH_2Cl_2, RT, 86%; (**d**) (i) **43**, TMSOTf, 4 Å MS, dichloroethane, RT, 80%; (ii) TBAF, AcOH, THF, RT, 95%

to the deschlorocallipeltoside aglycon (**75**) by Schmidt glycosidation (Scheme 13) [8, 35].

Deschlorocallipeltoside A was completed in two steps by attachment of trichloroacetimidate **43** to glycosyl acceptor **75** and subsequent deprotection using TBAF. The resulting ^{1}H and ^{13}C NMR data showed a striking similarity with callipeltoside A (**1**), except in the regions where the chlorine substituent would be present. This provided evidence that the relative configuration of the C1–C13 fragment with respect to the callipeltose A sugar was correct and would likely translate to the natural product following attachment of the correct *trans*-chlorocyclopropane moiety. Whilst this was a major milestone, the absolute stereochemistry of the natural product could not be inferred as the sign and magnitude of the optical rotation differed significantly [$[\alpha]_D = +45.0$ ($c = 0.50$, MeOH) verses $[\alpha]_D = -17.6$ ($c = 0.04$, MeOH) for callipeltoside A (**1**)] following omission of the chlorine substituent (see Sect. 2.1.4 for comment on the influence of the *trans*-chlorocyclopropane on the measured optical rotation) [35].

2.3 *Trost Synthesis of Callipeltoside A (2002)*

Following the synthesis of deschlorocallipeltoside A [35], Trost completed the first total synthesis of callipeltoside A [7, 8]. Prior to this, two stereochemical issues needed to be resolved: (1) the correct enantiomer of the *trans*-chlorocyclopropane

had to be determined by attachment to macrocycle **73** and (2) the absolute stereochemistry of the natural product deduced as a result [7, 8]. With this in mind, the initial synthetic strategy was executed in exactly the same way as for deschlorocallipeltoside A, with the only difference being the synthesis of the *trans*-chlorocyclopropane moiety.

2.3.1 Synthesis of Enantiomeric *trans*-Chlorocyclopropanes 84 and *ent*-84

Preparation of the *trans*-chlorocyclopropane commenced from bis-menthol compound **78**, which was commercially available as either enantiomer [7, 8]. Sequential deprotonation using LiTMP and addition of bromochloromethane gave *trans*-configured cyclopropane **79** in high diastereoselectivity (>99:1) after recrystallisation [7, 8]. Hydrolysis of a single ester group and acid chloride formation gave substrate **80** which, upon submission to a modified Barton–Crich–Motherwell decarboxylation procedure [40], provided the requisite *trans*-chlorocyclopropane geometry in good yield (60%) and diastereoselectivity (dr = 97:3) [7, 8]. A further three synthetic steps provided compound **37**, which underwent a one-pot Stille reaction/elimination sequence to incorporate the C16–C17 *trans*-double bond and internal alkyne [41]. Additional manipulation by means of an Appel reaction and displacement of the resulting bromide with $P(OEt)_3$ gave phosphonate coupling partner **84** in 10 linear steps and 20% overall yield (Scheme 14, one enantiomer shown for clarity) [7, 8].

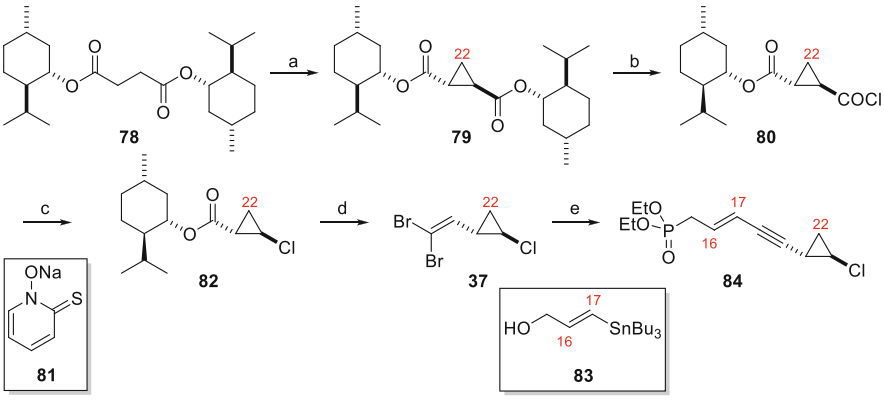

Scheme 14 Synthesis of the *trans*-chlorocyclopropane (one enantiomer shown). *Reagents and conditions*: (**a**) LiTMP, $BrCH_2Cl$, THF, −78°C, 87%, dr > 99:1 (following one crystallisation); (**b**) (i) NaOH, *i*-PrOH, 70°C; (ii) $SOCl_2$, RT, 90% (over 2 steps); (**c**) **81**, DMAP, TBAI, CCl_4 (0.02 M), RT, then AIBN, 80°C, 60%, dr = 97:3; (**d**) (i) HCl•HNMe(OMe), *i*-PrMgCl, THF, −10°C; (ii) DIBAL-H, CH_2Cl_2, −78°C; (iii) CBr_4, PPh_3, CH_2Cl_2, RT, 80% (over 3 steps); (**e**) (i) **83**, $[Pd_2dba_3]$•$CHCl_3$, $(4\text{-}OMeC_6H_4)_3P$, DIPEA, DMF, 80°C, 66%; (ii) CBr_4, PPh_3, CH_2Cl_2, −40°C, 90%; (iii) $P(OEt)_3$, 100°C, 93%

2.3.2 Completion of Callipeltoside A (1)

Phosphonate **84** and its enantiomer were appended to **73** via a Horner–Wadsworth–Emmons reaction. Subsequent deprotection and concomitant cyclisation then afforded diastereomeric aglycons **9** and **86** [7, 8], proceeding in near identical yield and selectivity to that previously reported for deschlorocallipeltoside A [35]. Once again the callipeltose A sugar **43** was attached by Schmidt glycosidation (Sect. 2.2.4), with deprotection using TBAF revealing callipeltoside diastereomers **85** and **7** (Scheme 15). Comparison of the ^{1}H and ^{13}C NMR spectra generated for these compounds with the natural isolate disappointingly revealed no significant differences [7, 8]. However, as previously noted by Paterson (Sect. 2.1.4) [17], the presence of the *trans*-chlorocyclopropane unit meant significantly different optical rotations for each diastereomer. An optical rotation of $[\alpha]_D^{22} = -19.2$ ($c = 1.0$, MeOH) was recorded for diastereomer **85**, whereas **7** was $[\alpha]_D^{22} = +156.3$ ($c = 0.55$, MeOH) [7, 8]. Comparison with the natural isolate [$[\alpha]_D^{22} = -17.6$ ($c = 0.04$, MeOH)] therefore suggested that diastereomer **85** was consistent with being callipeltoside A (**1**). Hence, the structural assignment of callipeltoside A was made possible purely by comparison of the sign and magnitude of the measured optical rotation [7, 8].

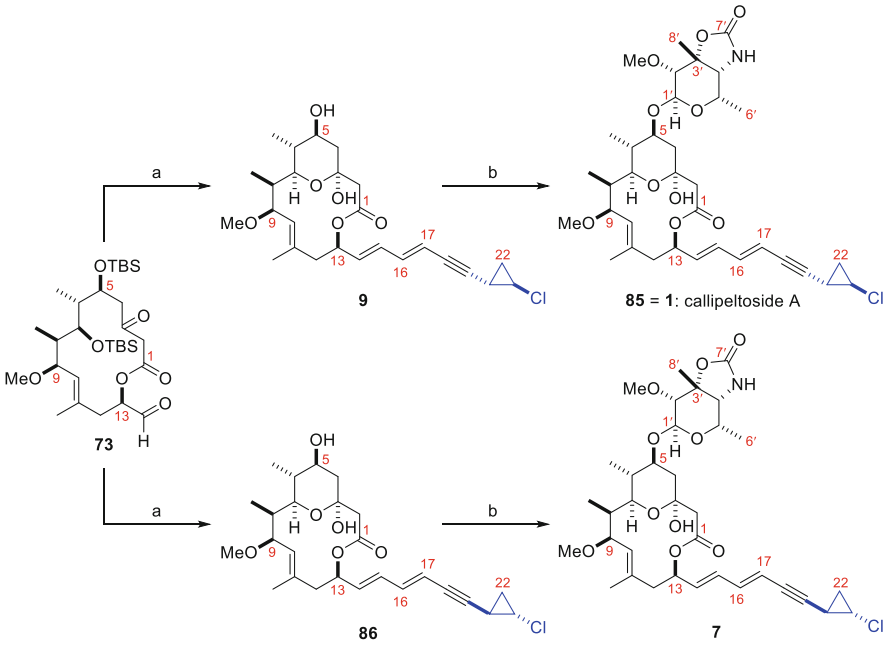

Scheme 15 Completion of callipeltoside A. *Reagents and conditions*: (**a**) (i) LiHMDS, **84** or *ent*-**84**, THF, −78°C to −40°C to RT, *E*:*Z* = 4:1; (ii) HF•pyridine, MeOH, 0°C, 50% (over 2 steps in both cases); (**b**) (i) **43**, TMSOTf, 4 Å MS, 1,2-dichloroethane, −30°C; (ii) TBAF, AcOH, THF, RT, 70% (over 2 steps in both cases)

Trost's synthesis of callipeltoside A was completed in a total of 50 manipulations, with 22 steps making up the longest linear sequence (0.47% overall yield) [7, 8]. Although the stereochemical uncertainties for callipeltoside A had been resolved, the group wanted to improve the diene-yne synthesis, as only 4:1 *E*:*Z* ratio (at C14–C15) was obtained from the earlier Horner–Wadsworth–Emmons reaction.

2.3.3 Second-Generation Synthesis of the Callipeltoside Aglycon 86

The second generation began with the interception of alkene **44** (Sect. 2.2.3), which was converted to the corresponding hemi-ketal **87** following TBS deprotection. Cross metathesis with crotonaldehyde in the presence of Grubbs' second-generation catalyst and subsequent Takai reaction provided vinyl iodide **88** in a significantly improved 8:1 *E*:*Z* ratio at C16–C17 (Scheme 16) [8]. At this point it was noted that volatile alkyne **12** (described by Paterson, Sect. 2.1.3) [17] was avoided for practical reasons, and so a one-pot reaction involving formation of the alkynyl stannane in situ and subsequent Stille coupling delivered **86**. This sequence represented an improvement on the step count and diene (*E*) selectivity of the first-generation synthesis, but was only reported with the oppositely configured *trans*-chlorocyclopropane (*ent*-**37**) (Scheme 16) [8].

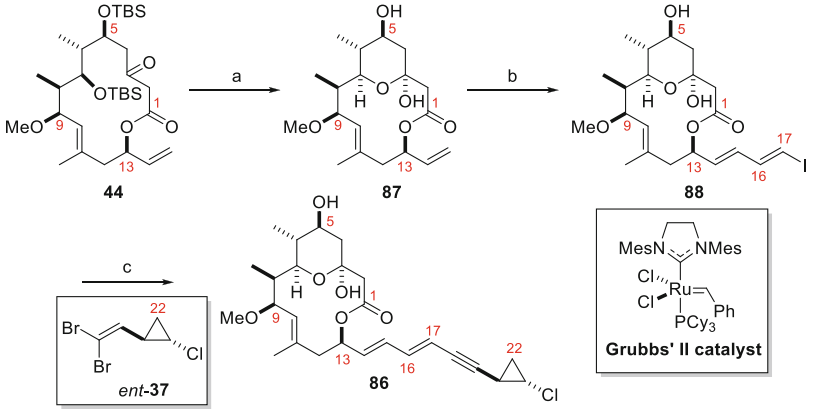

Scheme 16 Second-generation coupling of the *trans*-chlorocyclopropane. *Reagents and conditions*: (**a**) (i) HF•pyridine, MeOH, 0°C; (ii) PPTS, MeCN–H_2O (3:1), RT, 91% (over 2 steps); (**b**) crotonaldehyde, Grubbs' II, CH_2Cl_2, 40°C, then $CrCl_2$, CHI_3, dioxane–THF (4:1), 0°C, *E*:*Z* = 8:1, 84%; (**c**) *n*-BuLi, *ent*-**37**, Me_3SnCl, Et_2O, −78°C to RT, then **88**, $(MeCN)_2PdCl_2$ (3 × 10 mol%), DMF, RT, 70%

2.4 *Evans Synthesis of Callipeltoside A (2002)*

Shortly after Trost published the completion of callipeltoside A, Evans also disclosed the synthesis of the molecule [9, 10].

2.4.1 Retrosynthesis

The absolute configuration of callipeltoside A was not known at the start of the project, and so Evans applied a similar retrosynthetic approach whereby the *trans*-chlorocyclopropane was attached at a late stage. This was to be achieved by Horner–Wadsworth–Emmons reaction with sidechain **92**, enabling the stereochemistry of the sidechain to be deduced at a late stage [9, 10]. Sequential aldol reactions would be key for the synthesis of the C1–C13 fragment **91**, which would be completed by macrocyclisation to form the C13–O bond (Scheme 17).

2.4.2 Synthesis of C1–C13 Fragment 91

A copper-catalysed vinylogous aldol reaction between **95** and **96** set the (*R*)-configured C13 stereocentre and forged the C10–C11 trisubstituted double bond to give **98**

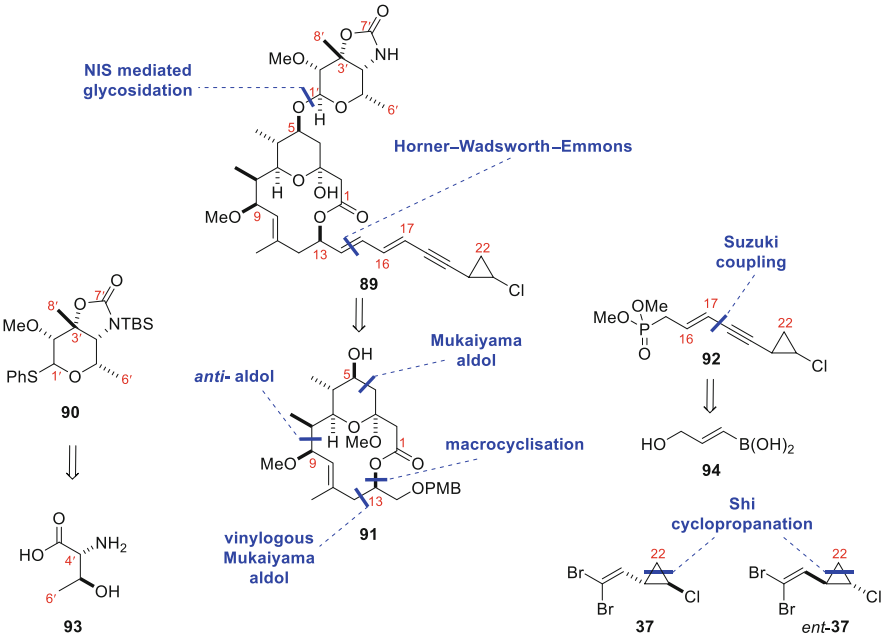

Scheme 17 Evans approach to callipeltoside A

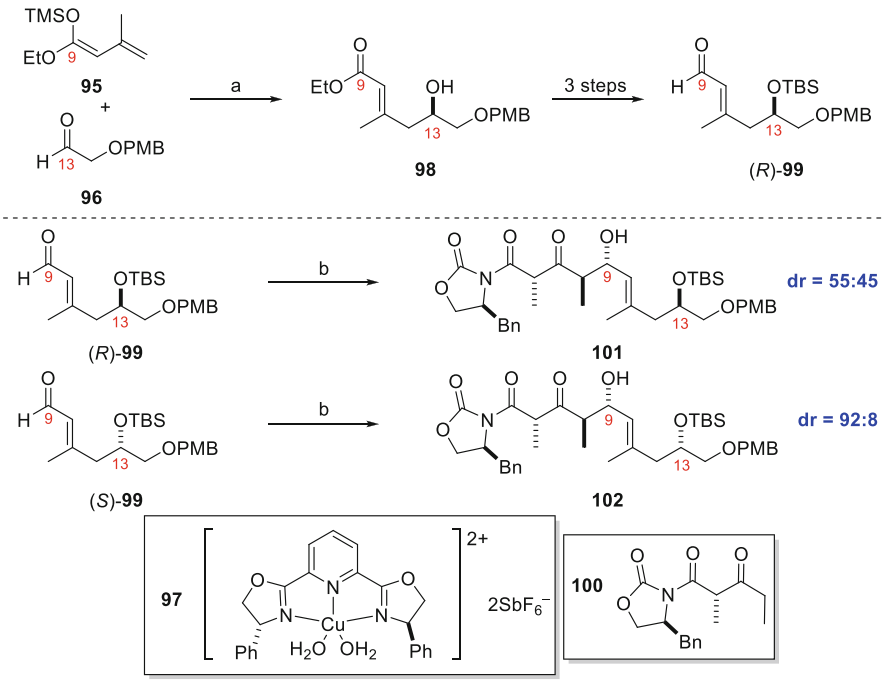

Scheme 18 Synthesis of the C5–C14 fragment. *Reagents and conditions:* (**a**) **97**, CH_2Cl_2, −78°C; 1 N HCl, EtOAc, RT, 93%, er = 97.5:2.5; (**b**) **100**, Cy_2BCl, $EtNMe_2$, Et_2O, 0°C to −78°C then RCHO, −78°C to −20°C

as a single isomer in 93% yield and high enantioselectivity (er = 97.5:2.5) (Scheme 18) [9, 10, 42]. Aldehyde **99** was then synthesised in a three-step protection, reduction and oxidation sequence.

Interestingly, aldol reaction between (*R*)-aldehyde **99** and oxazolidone **100** gave very poor diastereoselection in favour of the desired *anti*-product **101** (dr = 55:45). This was not the case when (*S*)-configured enantiomer **99** was subjected to the same conditions, with excellent diastereoselectivity (dr = 92:8) observed. As a result, the undesired C13 configured product **102** was carried through the synthesis with the need to invert this stereocentre at a later stage (Scheme 18) [9, 10].

Further routine manipulations followed by the addition of Chan's diene **104** under Felkin–Anh control resulted in **105** in excellent diastereoselectivity (dr > 95:5). Silylation, methanolysis and methylation then gave callipeltoside pyran **106**. The C13 stereocentre was then inverted using a four-step procedure involving selective TBS deprotection, mesylation (to give **107**), hydrolysis of the methyl ester and finally macrocycle formation. PMB-protected scaffold **91** was completed by treatment with TBAF (Scheme 19) [9, 10].

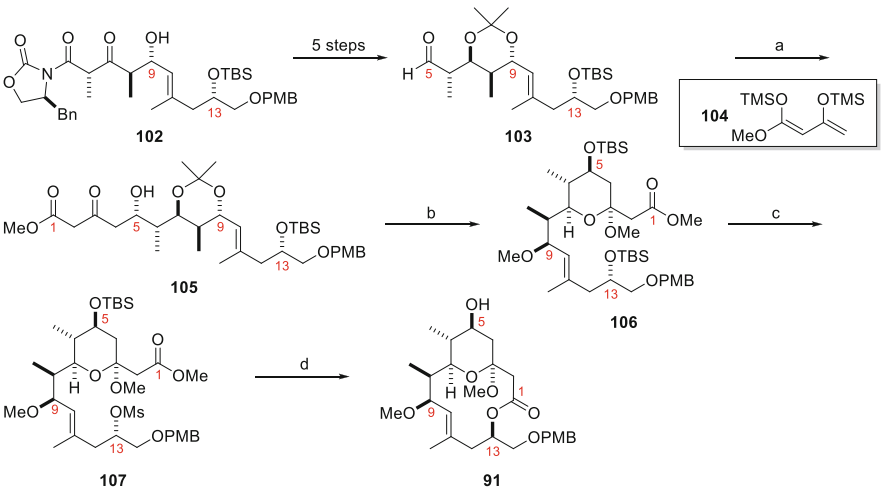

Scheme 19 Synthesis of C1–C13 macrocycle **91.** *Reagents and conditions:* (**a**) **104**, BF_3•OEt_2, PhMe, −90°C, 88%, dr > 95:5; (**b**) (i) TBSOTf, 2,6-lutidine, CH_2Cl_2, −78°C; (ii) PPTS, MeOH, RT; (iii) MeOTf, 2,6-di-*t*-butylpyridine, CH_2Cl_2, RT, 50% (over 3 steps); (**c**) (i) TBAF, THF, RT; (ii) MsCl, Et_3N, DMAP, CH_2Cl_2, 0°C; (iii) LiOH, H_2O, MeOH–THF (1:1), RT, 67% (over 3 steps); (**d**) (i) Cs_2CO_3, 18-crown-6, PhMe, 110°C; (ii) TBAF, THF, RT, 66% (over 2 steps)

2.4.3 Synthesis of *trans*-Chlorocyclopropane Sidechain 116

Similar to the Trost synthesis [7, 8], Evans designed the route to the *trans*-chlorocyclopropane unit to be flexible enough such that both enantiomers could be accessed (Scheme 20, desired enantiomer shown) [9, 10, 43]. Oxidative cleavage of **108** using KIO_4 provided aldehyde **109**, from which compound **112** could be produced using either a one- or two-step procedure. Although the Takai protocol resulted in vinyl chloride **112** in good stereoselectivity (*E*:*Z* = 6.7:1), this process was not ideal since it was difficult to separate the two isomers and only resulted in poor isolated yield (< 40%). This was remedied by use of a two-step sequential homologation (to alkyne **111**) and reduction sequence using the Ohira–Bestmann reagent (**110**), followed by Masuda's one-pot hydroboration/chlorination methodology [44]. This not only resulted in better double bond selectivity (*E*:*Z* > 20:1) but also improved overall yield (70%, **111** to **112**) [9, 10, 43].

The authors comment that cyclopropanation of vinyl chloride **112** was troublesome at first, with the traditional Simmons–Smith reaction as well as the modified variants developed by Furukawa (Et_2Zn, CH_2I_2) [45] and Denmark (Et_2Zn, CH_2I_2, ZnI_2) [46] all resulting in little or no product. However, the conditions developed by Shi (Et_2Zn, CH_2I_2, TFA) [47] gave **113** in good yield (82%) and excellent diastereoselectivity (dr > 98:2) [9, 10, 43]. Deprotection, oxidative cleavage of the resulting diol and dibromoolefination gave **37** (also used by Paterson [17] and Trost [7, 8]). This underwent Suzuki reaction with boronic acid **94** under Roush-modified

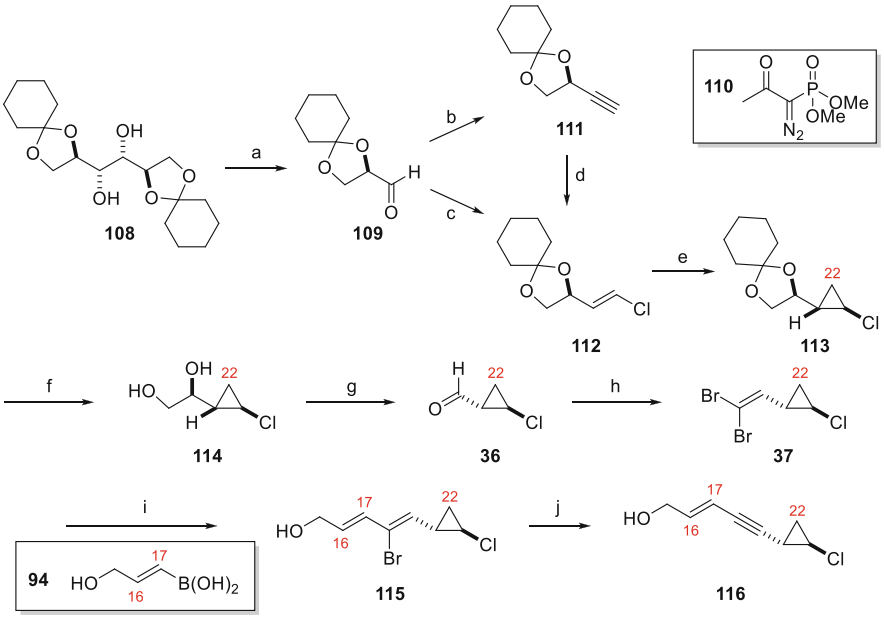

Scheme 20 Formation of *trans*-chlorocyclopropane fragment **116** (desired enantiomer). *Reagents and conditions*: (**a**) KIO_4, $KHCO_3$, H_2O–THF (3:1), RT; (**b**) **110**, K_2CO_3, MeOH, RT, 94% (over 2 steps); (**c**) $CrCl_2$, $CHCl_3$, THF, 70°C, < 40% (over 2 steps), *E*:*Z* = 6.7:1; (**d**) (i) $Thexyl_2BH$, −15°C to 0°C, THF, (ii) $CuCl_2$, H_2O, HMPA, THF, 0°C to 70°C, 70% (over 2 steps), *E*:*Z* > 20:1; (**e**) $ZnEt_2$, CF_3COOH, CH_2I_2, CH_2Cl_2, 0°C to RT, 82%, dr > 98:2; (**f**) Dowex resin, MeOH, RT, 84%; (**g**) $Pb(OAc)_4$, K_2CO_3, CH_2Cl_2, 0°C; (**h**) PPh_3, CBr_4, CH_2Cl_2, 0°C to RT, 94% (over 2 steps); (**i**) **94**, $Pd(PPh_3)_4$, TlOEt, THF–H_2O (3:1), RT, 85%; (**j**) DBU, PhMe, 110°C, 91%

conditions [48], with final elimination of HBr providing advanced fragment **116** in 33% overall yield (Scheme 20) [9, 10, 43].

2.4.4 L-Callipeltose A Sugar 90

Synthesis of the L-callipeltose A sugar began from D-threonine (**93**), which was converted into chiral substrate **118** in a three-step procedure [49]. The aldol reaction between **118** and the lithium enolate of **119** was performed in order to set the C2′ and C3′ stereocentres. However, whilst the desired C3′-stereocentre could be accessed using this method (consistent with Felkin–Anh selectivity), the undesired *syn* aldol adduct predominated (dr = 66:34), meaning poor selectivity for C2′ stereocentre formation (Scheme 21) [9, 10, 49]. This unexpected stereochemical outcome was hypothesised to be the result of chelation between the lithium and α-alkoxy substituent, thereby reinforcing the preference for the formation of an (*E*)-configured enolate. The relative configuration of the C2′ and C3′ stereocentres was determined by nOe studies following conversion of aldol adducts **120** and **122** to the

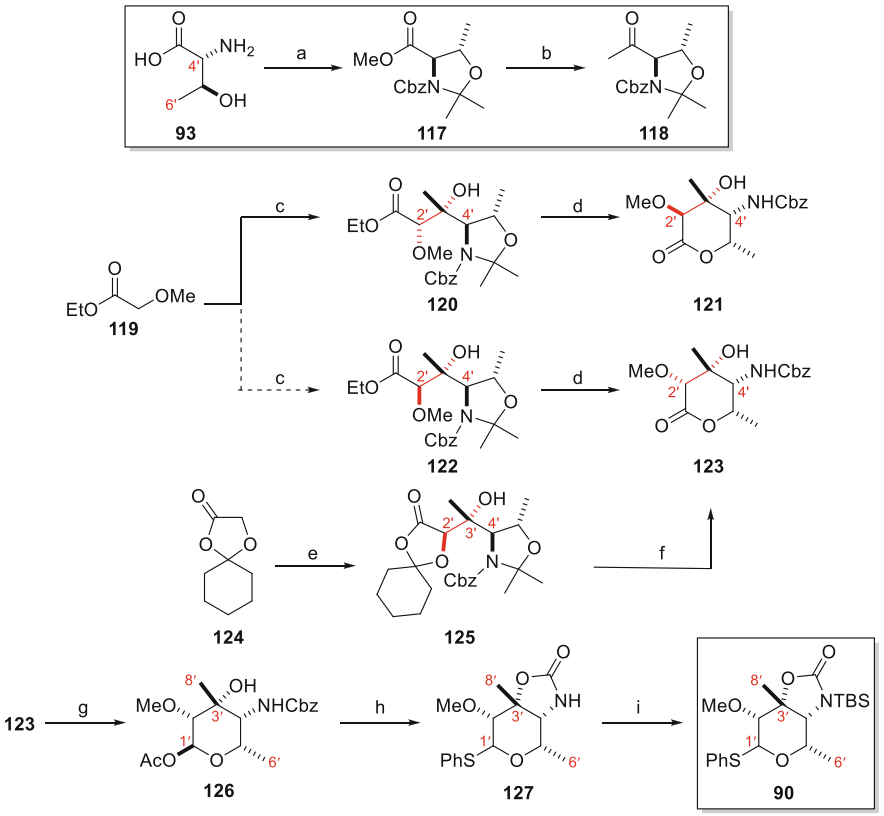

Scheme 21 Synthesis of L-callipeltose A (**90**). *Reagents and conditions*: (**a**) (i) 1 M NaOH, CbzCl, MeCN, 0°C to RT; (ii) MeI, K_2CO_3, DMF, 0°C to RT; (iii) TsOH•H_2O, 2,2-dimethoxypropane, PhH, RT, 93% (over 3 steps); (**b**) (i) *i*-PrMgCl, HN(OMe)Me•HCl, THF, −78°C to −40°C; (ii) MeMgBr, THF, −40°C to RT, 61% (over 2 steps); (**c**) LDA, then **118**, −78°C to −30°C, 56%, dr = 66:34; (**d**) HF, THF (no yield given); (**e**) LDA, then **118**, −78°C to −30°C, 80%, dr = 94:6; (**f**) (i) AcOH–H_2O (1.5:1), 70°C, 71%; (ii) Me_3OBF_4, DTBMP, CH_2Cl_2, RT, 82%; (**g**) DIBAL-H, CH_2Cl_2, −78°C, then Ac_2O, pyridine, DMAP, −78°C, 93%; (**h**) (i) BF_3•OEt_2, PhSH, CH_2Cl_2, 0°C to RT, 81%, α:β = 50:50; (ii) NaH, THF, 0°C to RT, 97%; (i) TBSOTf, 2,6-lutidine, CH_2Cl_2, 0°C to RT, 92%

corresponding lactones. In order to ensure formation of an enolate that could only exist in the (*Z*)-configuration (and therefore set the desired C2′ stereochemistry), the lithium enolate derived from **124** was studied. This resulted in formation of the correct Felkin–Anh *anti*-aldol adduct **125** in excellent yield (80%) and much-improved diastereoselectivity (dr = 94:6). With the desired C2′ stereochemistry set, conversion to lactone **123** followed by routine synthetic manipulations afforded thioglycoside **90** as a 50:50 mixture of α/β anomers (Scheme 21) [9, 10, 49].

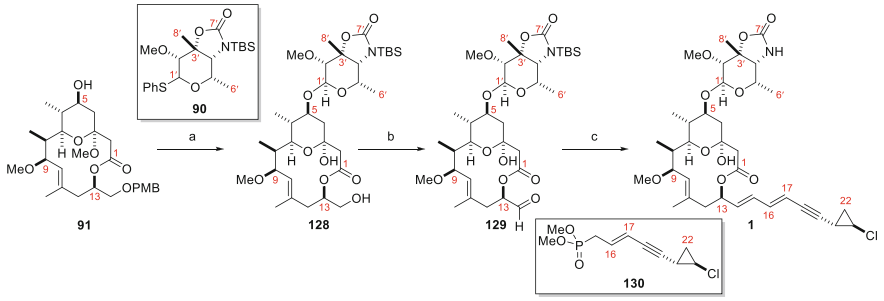

Scheme 22 Completion of callipeltoside A. *Reagents and conditions*: (**a**) (i) **90** (α/β = 50:50), NIS, TfOH, DTBMP, 4 Å MS, CH_2Cl_2, −15°C to RT; (ii) DDQ, MeOH, CH_2Cl_2–H_2O (1.3:1), RT, 83%; (**b**) SO_3•pyridine, Et_3N, DMSO, CH_2Cl_2, 0°C; (**c**) (i) LiHMDS, **130**, THF, −78°C to RT; (ii) I_2, CH_2Cl_2, RT, *E*:*Z* = 11:1; (iii) TBAF, AcOH, THF, RT, 56% (over 4 steps)

2.4.5 Completion of Callipeltoside A

In contrast to the callipeltoside A synthesis completed by Trost [7, 8], Evans appended the callipeltose A sugar prior to the *trans*-chlorocyclopropane [9, 10]. Glycosidation between thioglycoside **90** [as an anomeric mixture (α/β = 50:50)] and the C1–C13 core delivered the coupled material as a single product. Subsequent PMB deprotection and oxidation then gave aldehyde **129**. Horner–Wadsworth–Emmons reaction between **129** and **130** resulted in moderate *E*:*Z* selectivity at the C14/C15 *E*-olefin (3:1). Treatment of this mixture with a catalytic amount of iodine was thereafter found to result in isomerisation of the undesired *Z*-isomer, improving the ratio to 11:1. Final TBS deprotection then provided callipeltoside A (**1**) in 25 steps and 4.0% overall yield. The optical rotation of this synthetic material [$[\alpha]_D = -17$ ($c = 0.19$, MeOH)] was in full agreement with both the callipeltoside A natural isolate (Minale [3]) and that prepared by Trost (Scheme 22) [7, 8]. For completion, oppositely configured *trans*-chlorocyclopropane diastereomer **7** was also produced in an analogous fashion (not shown, also synthesised by Trost, Sect. 2.3.2), with the measured optical rotation having both different sign and magnitude [$[\alpha]_D = +140$ ($c = 0.05$, MeOH)] [9, 10].

2.5 Paterson Synthesis of Callipeltoside A (2003)

Paterson's synthesis of the enantiomeric callipeltoside aglycon **41** [17] (Sect. 2.1) was adapted for the synthesis of callipeltoside A. Key to this was the development of an asymmetric vinylogous Mukaiyama aldol reaction to set the C13 stereocentre. A chiral Lewis acid system requiring (*R*)-BINOL-Ti(O*i*-Pr)$_2$ [derived from (*R*)-BINOL and Ti(O*i*-Pr)$_4$] in the presence of CaH_2 provided trisubstituted alkene **133** in 94% yield and high enantioselectivity (er = 97:3). Further manipulation resulted in

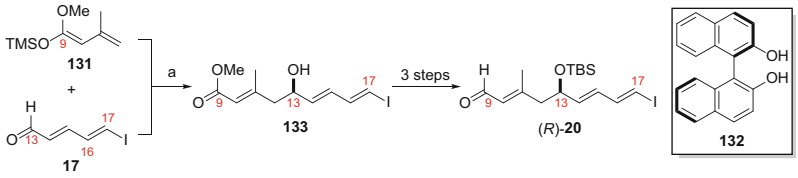

Scheme 23 Paterson's asymmetric synthesis of (*R*)-**20.** *Reagents and conditions*: (**a**) CaH_2, (*R*)-BINOL, **132**, Ti(O*i*-Pr)$_4$, THF, RT, then −78°C, aldehyde **17**, followed by silyl ketene acetal **131**, 96%, er = 97:3

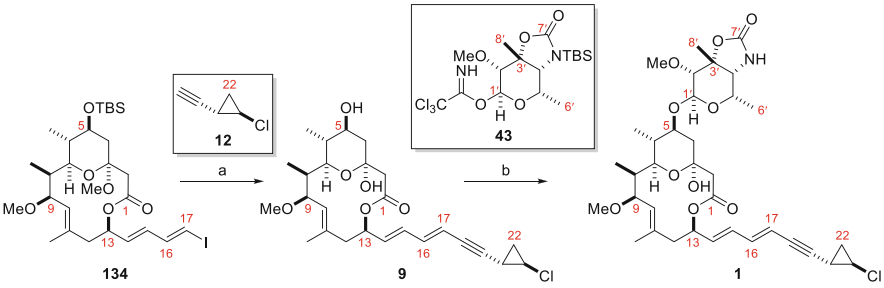

Scheme 24 Completion of callipeltoside A. *Reagents and conditions*: (**a**) (i) **12**, $Pd(PPh_3)_2Cl_2$, CuI, *i*-Pr_2NH, EtOAc, −20°C to 0°C, 83%; (ii) TFA, aq. THF, RT, 98%; (**b**) (i) **43**, TMSOTf, CH_2Cl_2, 4 Å MS, −30°C; (ii) TBAF, AcOH, THF, RT, 76% (over 2 steps)

aldehyde (*R*)-**20**, allowing for the interception of the analogous enantiomeric route (Sect. 2.1) (Scheme 23) [11].

The callipeltoside aglycon was completed in the same manner as the enantiomeric version previously shown in Sect. 2.1.4. The callipeltose A sugar was synthesised following the procedure reported by Guiliano [25] and the corresponding trichloroacetimidate coupling partner **43** attached using Schmidt glycosidation conditions (analogous to Trost; see Sect. 2.2.4) [7, 8]. TBS deprotection with TBAF then gave callipeltoside A in 23 steps (longest linear) and 4.8% overall yield (Scheme 24) [11].

2.6 Panek Synthesis of Callipeltoside A (2004)

2.6.1 Retrosynthesis

The fourth synthesis of callipeltoside A was completed by Panek in 2004 [12]. Since the absolute and relative stereochemistry of callipeltoside A had been confirmed at this point, late-stage installation of the *trans*-chlorocyclopropane was not required. Instead, the Panek group sought to unite fully assembled C11–C22 fragment **136** with pyran core **135** by means of a Julia–Kocienski olefination, forming the

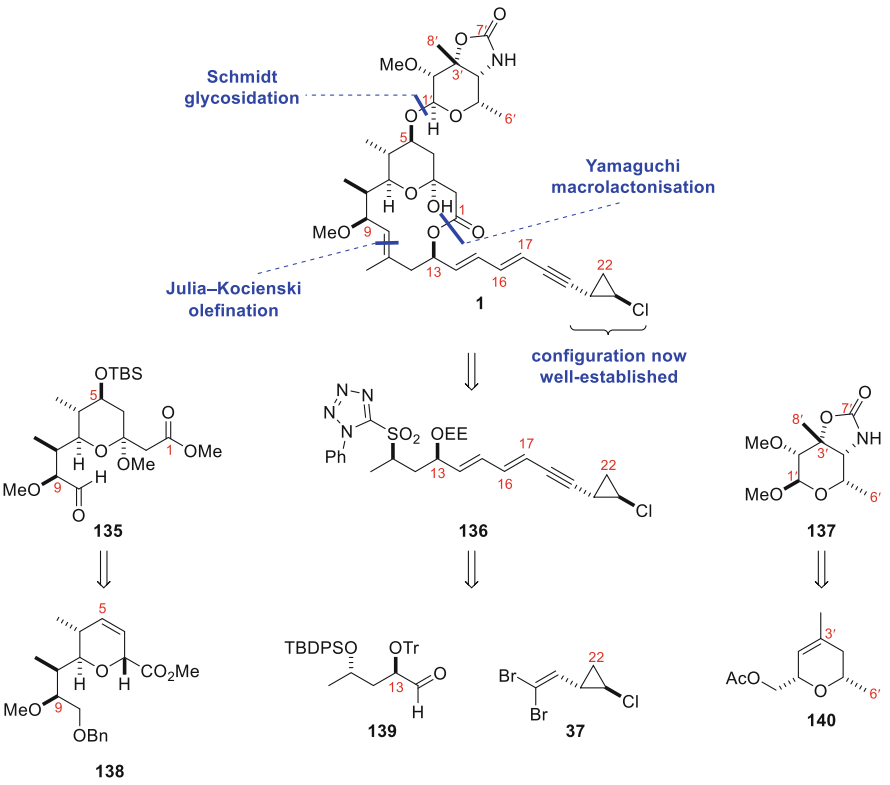

Scheme 25 Panek retrosynthesis of callipeltoside A

trisubstituted C10/C11 olefin in the process. In contrast to previous syntheses, pyran **135** and callipeltose A sugar **137** were to be derived from the relevant dihydropyrans arising from [4 + 2] annulations using chiral organosilanes (Scheme 25) [12, 50].

2.6.2 Formation of C1–C10 Pyran 135

The synthesis began with the installation of the C8 and C9 stereocentres via the *anti*-selective condensation of α-benzyloxyacetaldehyde **141** with chiral silane (*S*)-**142** in the presence of $SnCl_4$. This provided tetrahydrofuran **143** in high yield (87%) and diastereoselectivity (dr > 97:3). Treatment with $SbCl_5$ resulted in elimination and the formation of the *anti*-homoallylic alcohol, which could be converted to aldehyde **144** by methylation and ozonolysis. At this point aldehyde **144** could be reacted with chiral organosilane **145** in the presence of TfOH to afford tetrahydropyran **138** in 85% yield and as a single diastereomer (dr > 97:3). This was then converted to advanced pyranone **146** in a further three steps (Scheme 26) [12].

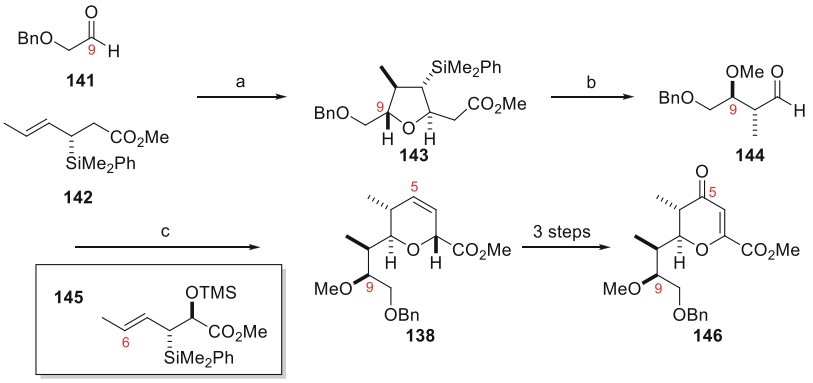

Scheme 26 Synthesis of the C1–C10 scaffold. *Reagents and conditions:* (**a**) **141**, $SnCl_4$, CH_2Cl_2, then **142**, CH_2Cl_2, −78°C, 87%, dr > 97:3; (**b**) (i) $SbCl_5$, CH_2Cl_2, −78°C to −50°C; (ii) Me_3OBF_4, proton sponge, 4 Å MS, CH_2Cl_2, RT; (iii) O_3, MeOH–CH_2Cl_2 (3:1), Me_2S, −78°C, 81% (over 3 steps); (**c**) **145**, TfOH, CH_2Cl_2, −70°C, 85%, dr > 97:3

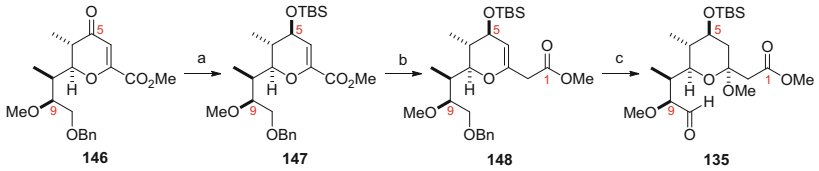

Scheme 27 Completion of pyran **135.** *Reagents and conditions:* (**a**) (i) $CeCl_3$•$7H_2O$, MeOH, −78°C, then $NaBH_4$, MeOH, −78°C, 93%; (ii) TBSOTf, 2,6-lutidine, CH_2Cl_2, −78°C, 97%; (**b**) (i) LiOH, THF–MeOH–H_2O (3:1:1), RT, then 5% HCl; (ii) $(COCl)_2$, DMF, CH_2Cl_2; (iii) CH_2N_2, Et_2O, 0°C, 70% (over 3 steps); (iv) $PhCO_2Ag$, pyridine, MeOH, RT, 80%; (**c**) (i) CSA, MeOH, RT, 97%; (ii) H_2, Pd/C, EtOAc; (iii) PDC, 4 Å MS, CH_2Cl_2, RT, 88% (2 steps)

Luche reduction provided the C5 stereocentre, and the resulting hydroxy was protected as its TBS-ether (**147**). The C1–C10 scaffold was then further manipulated by ester saponification and Arndt–Eistert homologation to give **148** in four steps and 56% overall yield. Installation of the anomerically favoured ketal (MeOH/CSA), Bn deprotection and oxidation then afforded aldehyde **135** (Scheme 27) [12].

2.6.3 Synthesis of the C11–C22 Fragment

Panek chose to assemble the entire C11–C22 fragment prior to coupling with aldehyde **135**.

The synthesis again required dibromoolefin **37** as a key building block, which was synthesised as described by Paterson [11, 17] (Sect. 2.1.3). This underwent Stille reaction using the conditions developed by Shen [41] (and also used by Olivo [20] and Trost [8]) to give enyne **116**, from which phosphonate **84** was prepared in a further two-step procedure (Scheme 28). Horner–Wadsworth–Emmons reaction

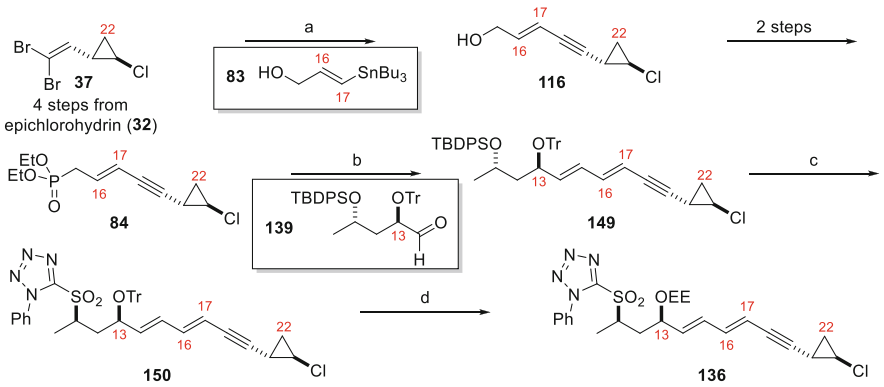

Scheme 28 Completion of the C11–C22 fragment. *Reagents and conditions*: (**a**) **83**, Pd_2dba_3, $(4\text{-}MeOC_6H_4)_3P$, DIPEA, DMF, 80°C, 68%; (**b**) LiHMDS, then **139**, THF, −78°C, 89%; (**c**) (i) TBAF, THF, RT, 91%; (ii) 1-phenyl-1*H*-tetrazole-5-thiol, DIAD, PPh_3, THF, 0°C to RT; (iii) $(NH_4)_6Mo_7O_{24}$, EtOH–acetone (2:1), RT, 66% (2 steps); (**d**) (i) TsOH, MeOH, RT; (ii) EVE, PPTS, RT, 90% (2 steps)

between phosphonate **84** and aldehyde **139** under identical conditions to Trost [8] interestingly resulted in the formation of a single *E*,*E*-isomer, highlighting the sensitivity of this reaction to substrate choice (Trost observed a 4:1 *E*/*Z* mixture when the coupling was performed with the callipeltoside C1–C13 macrocycle). With the entire C11–C22 carbon scaffold in place, the TBDPS group was removed and stereocentre inverted by Mitsunobu reaction with 1-phenyl-1*H*-tetrazole-5-thiol. Oxidation to the corresponding sulfone followed by protecting group manipulation gave Julia–Kocienski coupling partner **136** (Scheme 28) [12].

2.6.4 Synthesis of Callipeltose A

Organosilane methodology was also used to access the callipeltose A sugar [12, 51]. Stereoselective [4 + 2] annulation between acetaldehyde and chiral organosilane **151** (made in 5 steps, 55%) gave dihydropyran **140** in high yield and diastereoselectivity (dr = 10:1). This was converted to **152** in a further two steps, with selective reduction and methanolysis providing **153** as a single anomer. Advanced intermediate **155** was then constructed in short order by Sharpless dihydroxylation, selective methylation and carbamate formation. 1,5-C–H insertion using $Rh_2(OAc)_4$ then forged the requisite 5-membered ring present in callipeltose A in 93% yield (Scheme 29) [12, 51].

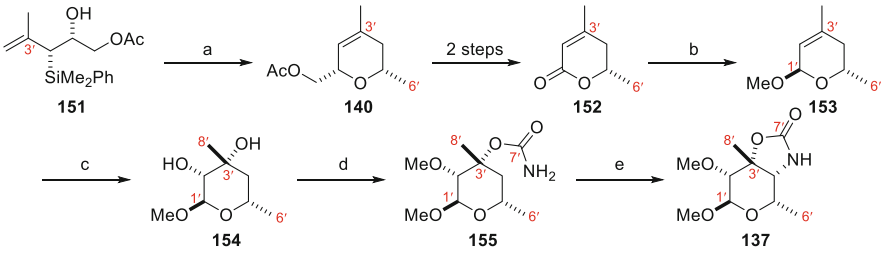

Scheme 29 Synthesis of the callipeltose A scaffold (**137**). *Reagents and conditions*: (**a**) MeCHO, TMSOTf, CH_2Cl_2, −78°C, dr = 91:9, 80%; (**b**) DIBAL-H, CH_2Cl_2, −78°C, then CSA, MeOH; (**c**) AD-mix-α, $NaHCO_3$, $MeSO_2NH_2$, OsO_4, *t*-BuOH–H_2O (1:1), RT, 65% (over 2 steps); (**d**) (i) *t*-BuOK, MeI, THF, 0°C; (ii) $Cl_3CCONCO$, CH_2Cl_2, RT, then K_2CO_3, MeOH–H_2O (10:1), 79% (over 2 steps); (**e**) $Rh_2(OAc)_4$, $PhI(OAc)_2$, MgO, PhH, 80°C, 93%.

2.6.5 Completion of Callipeltoside A

Aldehyde **135** and sulfone **136** were coupled using a Julia–Kocienski olefination to afford **156** in low yield (20%) after acidic cleavage of the ethoxyethyl ether (EE) protecting group. The yield could not be improved despite further investigation involving different bases (KHMDS, NaHMDS) and more polar solvents (DME, DMF) [12].

Hydrolysis of the ester group in **156** was followed by Yamaguchi macrolactonisation, which gave **157** as well as eliminated product **158** in a 50:50 ratio These products were separated and **157** processed by deprotection and hemi-ketal installation to give the callipeltoside aglycon (**9**).[2] This was then coupled to trichloroacetimidate **43** using the literature known Schmidt glycosidation conditions to give callipeltoside A (**1**) in 1.4% overall yield and 25 steps (longest linear) (Scheme 30) [12].

2.7 Hoye Synthesis of Callipeltoside A (2010)

2.7.1 Retrosynthesis

The synthesis of callipeltoside A was disclosed by Hoye in 2010 [13]. Similar disconnections involving late-stage attachment of the callipeltose A sugar via a Schmidt glycosidation and Horner–Wadsworth–Emmons reaction with phosphonate **84** were key to the assembly of callipeltoside A. However, a dual macrocyclisation/hemi-ketal formation process from acylketene precursor **161** was anticipated to form the C1–C13 macrocycle in one step. This precursor was to be accessed by alkenyllithium addition to aldehyde **163** (Scheme 31) [13, 52, 53].

[2]The undesired lactone (**158**) was recycled in two steps to provide additional quantities of the callipeltoside aglycon (**9**) (conditions shown in Scheme 30).

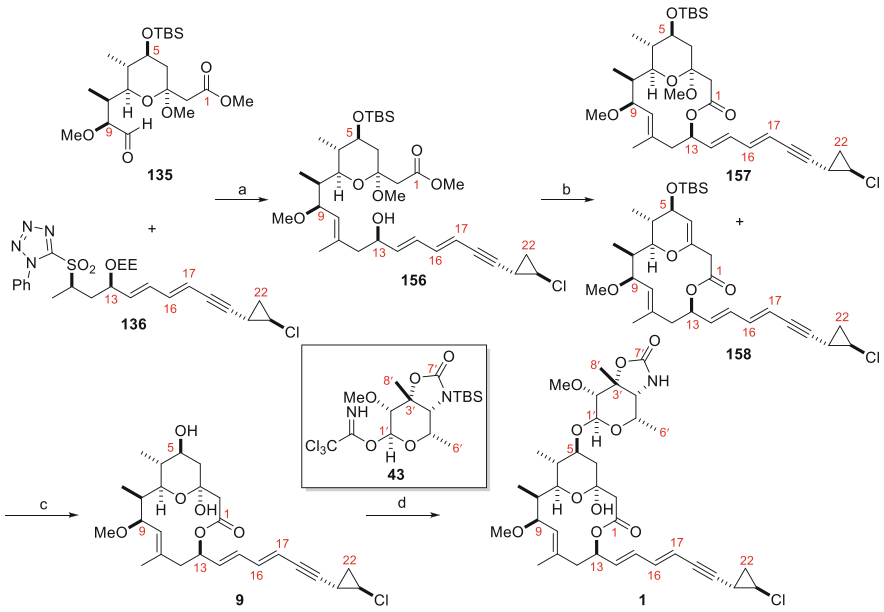

Scheme 30 Completion of callipeltoside A. *Reagents and conditions*: (**a**) (i) **136**, LiHMDS, then **135**, THF, −78°C to RT; (ii) PPTS, MeOH, 20% (over 2 steps); (**b**) (i) LiOH, MeOH–H_2O–THF, 90%; (ii) 2,4,6-$Cl_3C_6H_2COCl$, Et_3N, DMAP, PhMe, 80°C, 90% (**157** and **158**, 1:1); [**158** to **9** conversion: (i) PPh_3•HBr, H_2O–CH_2Cl_2 (11:1), RT, 97%; (ii) TBAF, THF, RT, 85%]; (**c**) (i) TBAF, THF, RT, 85%; (ii) PPTS, MeCN–H_2O (3:1), RT, 89%; (**d**) (i) **43**, TMSOTf, 4 Å MS, CH_2Cl_2, −30°C; (ii) TBAF, AcOH–THF (1:1), RT, 73% (over 2 steps)

2.7.2 Synthesis of the C1–C13 Fragment

Lithium-halogen exchange with vinyl iodide **162** followed by addition to aldehyde **163** gave a 50:50 mixture of separable C9 epimeric alcohols.[3] Methylation of the desired C9 alcohol afforded **164**, which was converted to lactonisation precursor **161** in an additional five linear steps (Scheme 32) [13].

Substrate **161** underwent the desired dual macrolactonisation/hemi-ketal formation process to afford the C1–C13 macrocyclic core **160** in 76% yield. This reaction was proposed to proceed via intermediates **165**, **166** and **167** (Scheme 33) [13, 53].

2.7.3 Completion of Callipeltoside A

Compound **168** was synthesised following a three-step protecting group manipulation. Subsequent oxidation to the aldehyde, coupling to phosphonate **84** and

[3]The undesired C13 epimer was oxidised and diastereoselectively reduced to afford additional quantities of **164**.

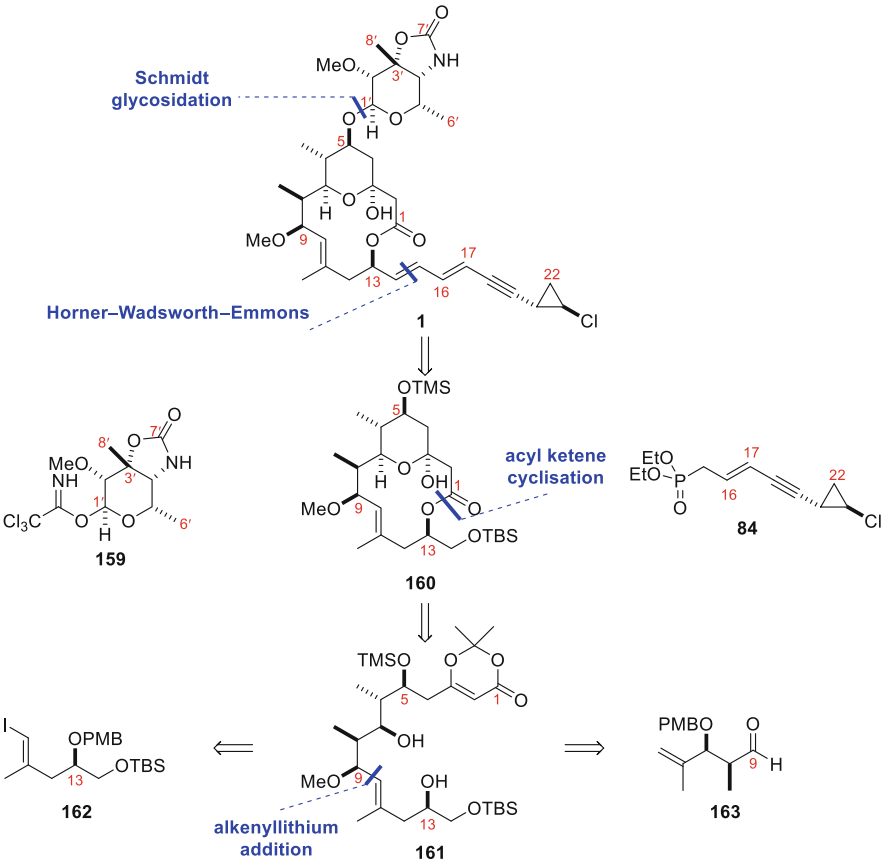

Scheme 31 Hoye's approach to callipeltoside A

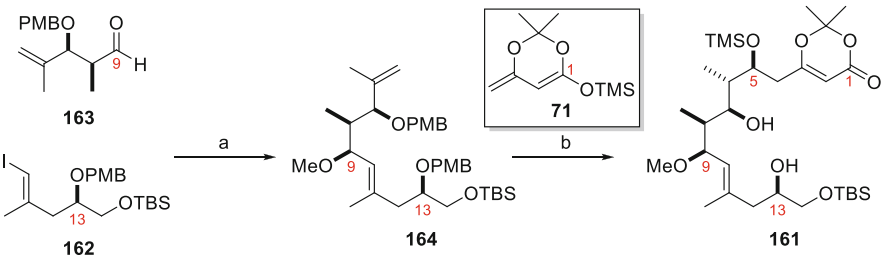

Scheme 32 Synthesis of cyclisation precursor **161.** *Reagents and conditions*: (**a**) (i) *n*-BuLi, **162**, Et_2O, −78°C, then **163**, Et_2O, dr = 50:50 (separation by SiO_2 chromatography), 34% of each; (ii) MeI, NaH, DMF, RT, 80%; (**b**) (i) 9-BBN, THF, −78°C to RT, then NaOH (10%)–H_2O_2 (30%) (6:1), 70%, dr = 87.5:12.5 (at C6, separation by SiO_2 chromatography); (ii) Dess–Martin periodinane, CH_2Cl_2, RT, 76%; (iii) **71**, BF_3•OEt_2, CH_2Cl_2, −78°C, 90%; (iv) TMSCl, Et_3N, CH_2Cl_2, RT; (v) DDQ, CH_2Cl_2–H_2O (12:1), 78% (over 2 steps)

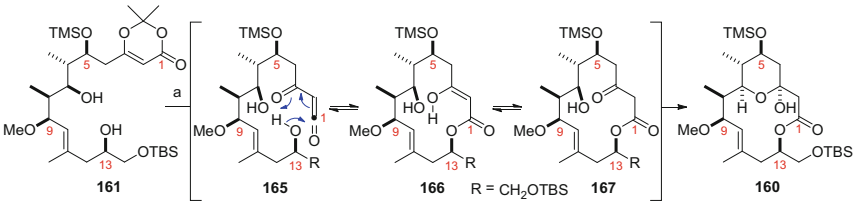

Scheme 33 Key dual macrocyclisation/hemi-ketal formation reaction [13, 53]. *Reagents and conditions*: (**a**) PhH, Δ, 76%

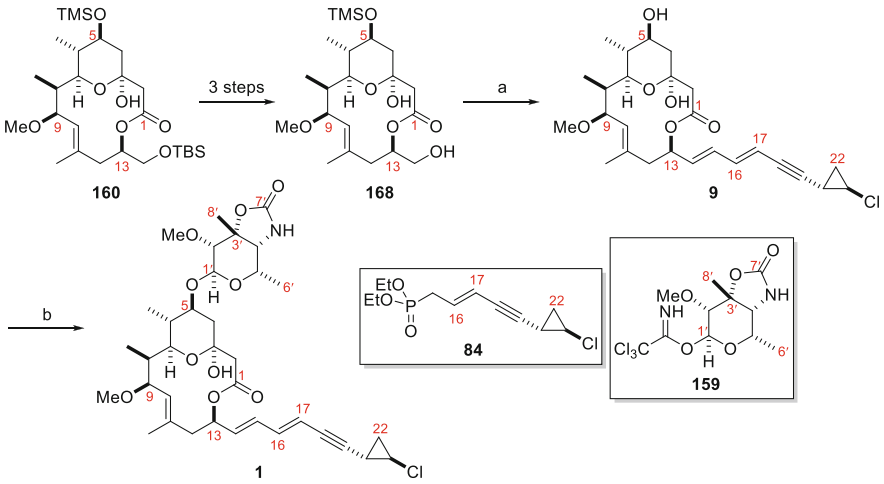

Scheme 34 Completion of callipeltoside A. *Reagents and conditions*: (**a**) (i) SO_3•pyridine, DMSO, Et_3N, CH_2Cl_2, 0°C; (ii) **84**, LiHMDS, THF, −78°C; (iii) TBAF, THF, 54% (over 3 steps); (**b**) **159**, TMSOTf, 4 Å MS, CH_2Cl_2, 0°C, 70%

deprotection gave the familiar callipeltoside aglycon (**9**). In accordance with previous syntheses, the trichloroacetimidate of callipeltose A sugar **159** (although with an exposed NH this time) was attached to **9** using Schmidt conditions, delivering the natural product in 21 steps and 0.7% yield (Scheme 34) [13].

2.8 *MacMillan Synthesis of Callipeltoside C (2008)*

2.8.1 Retrosynthesis

The first synthesis of callipeltoside C was reported in 2008 by MacMillan [16]. At this stage the relative configuration of callipeltose C with respect to the callipeltoside aglycon had not been validated, and therefore the absolute configuration of the molecule was not known [4]. In contrast to previous approaches towards these

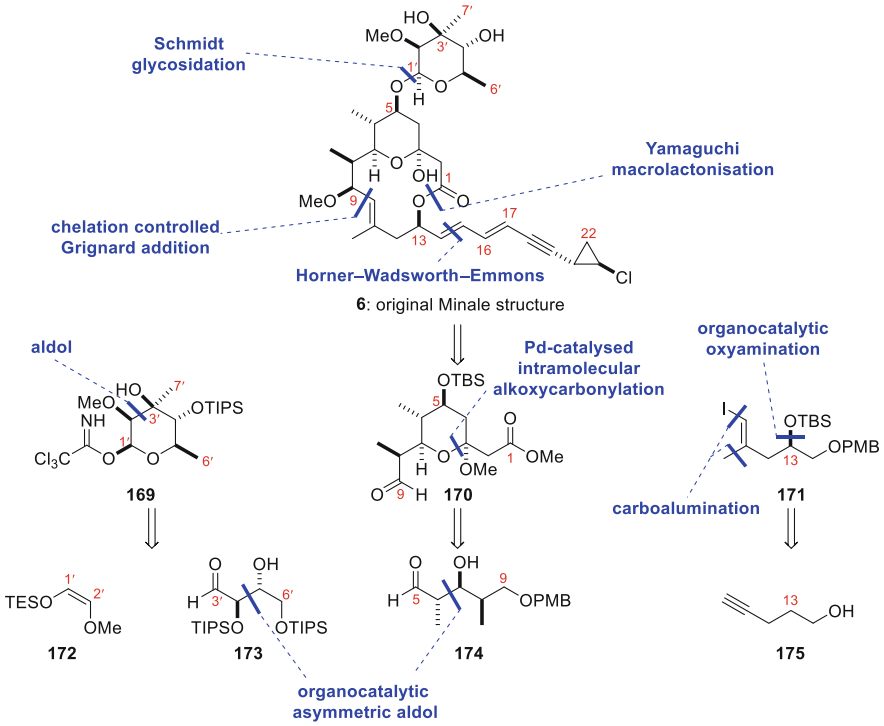

Scheme 35 Retrosynthesis of callipeltoside C

molecules, organocatalytic processes featured heavily in MacMillan's synthesis. Pyran **170** and callipeltose C sugar **169** were to be accessed using organocatalytic asymmetric aldol reactions, whilst the C13 stereocentre of **171** was to be set by an organocatalytic oxyamination reaction (Scheme 35) [16, 54–58].

2.8.2 Synthesis of Pyran 170

The synthesis began with an L-proline-catalysed organocatalytic aldol reaction between propionaldehyde (**176**) and Roche ester-derived aldehyde **177**. This gave aldehyde **174** in moderate yield (48%), but set the desired C6 and C7 stereocentres in both excellent diastereo- (dr = 92:8) and enantioselectivity (er > 99:1) [16]. The C5 stereocentre was then formed by propargylzinc addition to give the desired 1,3-*anti*-diol relationship (**180**, dr = 86:14). With the 4 contiguous C5–C8 stereocentres in place, a palladium-catalysed alkoxycarbonylation process developed by Marshall [59, 60] impressively gave advanced C1–C9 pyran **181** as a single diastereomer in one step (Scheme 36). The proposed mechanism for this transformation is described in Scheme 37 [59, 60]. Subsequent TBS protection of the C5 hydroxy, PMB removal and Parikh–Doering oxidation then gave **170** in six steps and 44% overall yield from aldehyde **177** (Scheme 36).

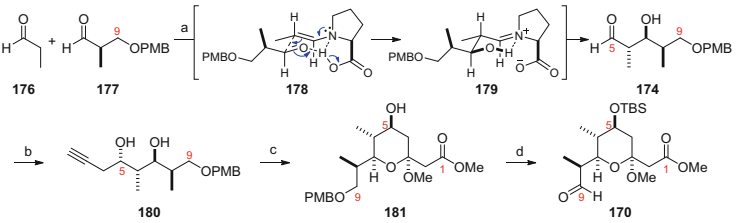

Scheme 36 Synthesis of pyran **170.** *Reagents and conditions:* (**a**) L-proline (10 mol%), DMSO, H_2O, 4°C, 48% (75% brsm), dr = 92:8 (*syn*:*anti*), er > 99:1; (**b**) $HCCCH_2Br$, Zn, THF, −100°C, 98%, dr = 86:14; (**c**) $PdCl_2(MeCN)_2$ (5 mol%), *p*-benzoquinone, CO, MeOH, 0°C, 75%, dr > 95:5; (**d**) (i) TBSCl, imidazole, DMF, RT; (ii) DDQ, pH 7 phosphate buffer, CH_2Cl_2, 0°C; (iii) SO_3•pyridine, Et_3N, CH_2Cl_2, DMSO, 0°C, 80% (over 3 steps)

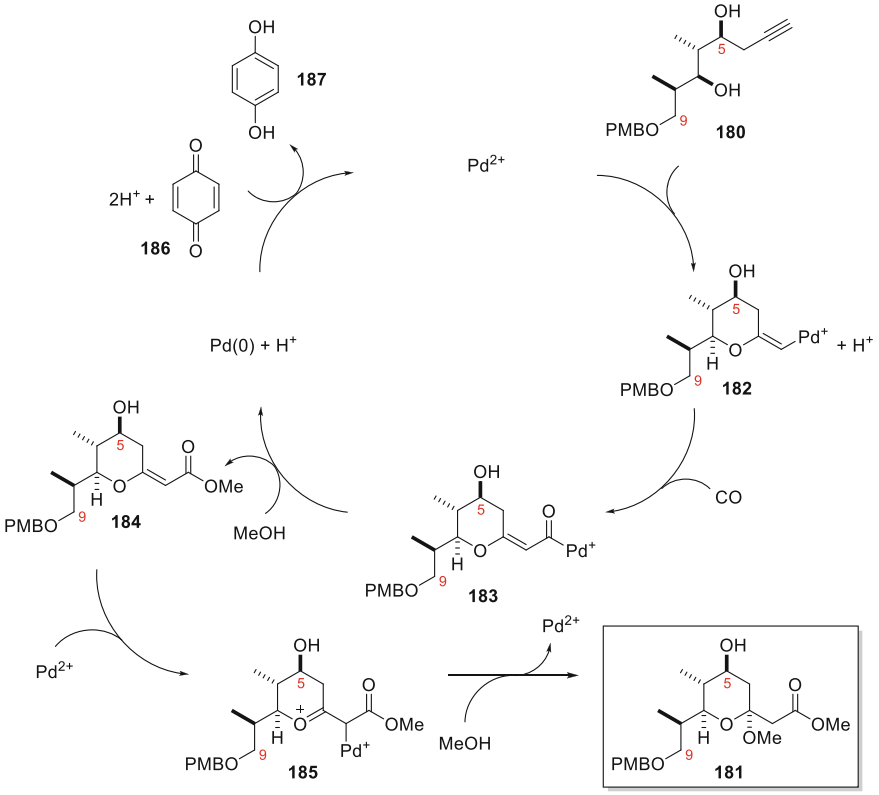

Scheme 37 Proposed mechanism for the palladium-catalysed alkoxycarbonylation reaction [59, 60]

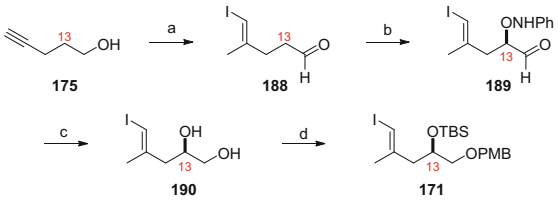

Scheme 38 Organocatalytic oxyamination approach to vinyl iodide **171.** *Reagents and conditions*: (**a**) (i) Me_3Al, Cp_2ZrCl_2, I_2, THF, −30°C; (ii) $(COCl)_2$, Et_3N, DMSO, CH_2Cl_2, −50°C, 92% (over 2 steps); (**b**) L-proline, (20 mol%), PhNO, DMSO, RT, er > 99:1; (**c**) (i) $NaBH_4$, EtOH, RT; (ii) Zn, EtOH–AcOH (3:1), 77% (over 3 steps); (**d**) (i) $Bu_2Sn(OMe)_2$, PMBCl, TBAI, PhMe, Δ; (ii) TBSCl, imidazole, DMF, RT, 80% (over 2 steps), er > 99:1

2.8.3 Formation of Vinyl Iodide 171

Carboalumination of 4-pentyn-1-ol delivered the desired trisubstituted double bond as a single regioisomer which, following treatment with iodine, gave **188**. Subsequent Swern oxidation and organocatalytic α-oxyamination then provided **189** in excellent enantioselectivity (er > 99:1) [57, 58]. Reduction of the aldehyde, N–O bond cleavage and bis-protection gave **171** in seven steps and 57% yield (Scheme 38) [16].

2.8.4 Fragment Union and Completion of the Aglycon (9)

Vinylic iodide **171** (2.2 equiv.) was converted to the corresponding Grignard and added to aldehyde **170** to provide the C9 stereocentre in both high diastereoselectivity (dr = 94:6) and yield (98%). The addition of $MgBr_2$ to substrate **170** prior to Grignard addition was found to be important for both yield and diastereoselectivity, with formation of a complex between $MgBr_2$ and the pyran and aldehyde oxygens speculated. It is also noted that an intermolecular Nozaki–Hiyama–Kishi reaction was also attempted and in contrast gave the undesired C9 alcohol configuration [16].

With **191** in hand, methylation, PMB deprotection, oxidation and Horner–Wadsworth–Emmons olefination with *trans*-chlorocyclopropane-containing phosphonate **130** gave **193** [16]. Interestingly, attachment of **130** at this stage of the synthesis resulted in high *E*:*Z* selectivity (10:1–19:1) compared to Trost [7, 8], Evans [9, 10] and Paterson [11] and once again highlights the subtleties associated with substrate choice when performing reactions under similar conditions (see Sects. 2.2.3, 2.3.2 and 2.4.5; *E*:*Z* = 4:1).

Deprotection of C13-OTBS and saponification of the methyl ester gave *seco*-acid **193** which, when subjected to Yamaguchi macrocyclisation conditions, gave eliminated lactone **158** as well as the desired product (**157**, not shown; see Sect. 2.6.5). Treatment of the mixture with aqueous PPh_3•HBr then installed the hemi-ketal functionality, whilst final TBS deprotection using TFA delivered the callipeltoside aglycon (**9**) in 18 steps and 19% overall yield (Scheme 39) [16].

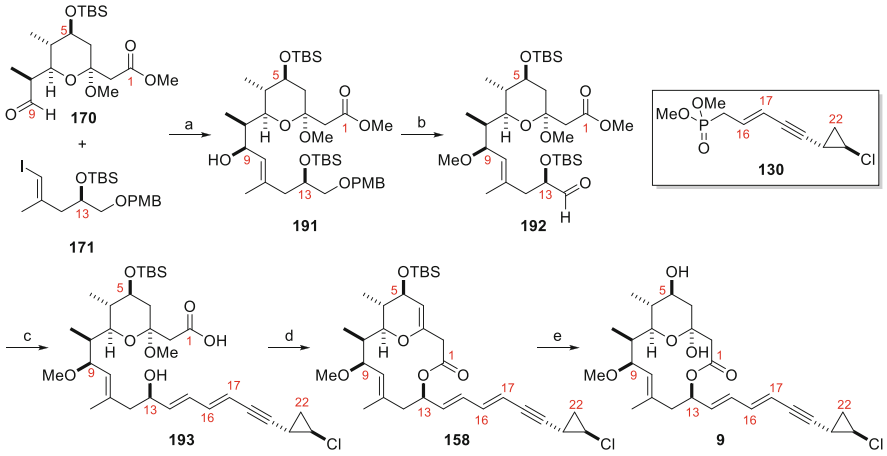

Scheme 39 Synthesis of callipeltoside aglycon (**9**). *Reagents and conditions*: (**a**) **171**, *t*-BuLi, $MgBr_2$•Et_2O, Et_2O, then **170**, CH_2Cl_2, −78°C, 98%, dr = 94:6; (**b**) (i) MeOTf, 2,6-di-*t*-butylpyridine, CH_2Cl_2, RT; (ii) DDQ, pH 7 buffer, CH_2Cl_2, 0°C; (iii) SO_3•pyridine, Et_3N, DMSO, CH_2Cl_2, −10°C, 84% (over 3 steps); (**c**) (i) **130**, LiHMDS, THF, −78°C, then **192**, THF, −78°C, 84%, *E*:*Z* = 19:1; (ii) TBAF, THF, 0°C, 100%; (iii) $Ba(OH)_2$•$8H_2O$, MeOH, RT, 84% (over 3 steps); (**d**) 2,4,6-$Cl_3C_6H_2COCl$, DIPEA, THF, RT, then addition to DMAP, PhMe, 60°C, 83%; (**e**) (i) PPh_3•HBr, H_2O, CH_2Cl_2, RT; (ii) TFA, THF–H_2O (5:1), RT, 81% (over 2 steps)

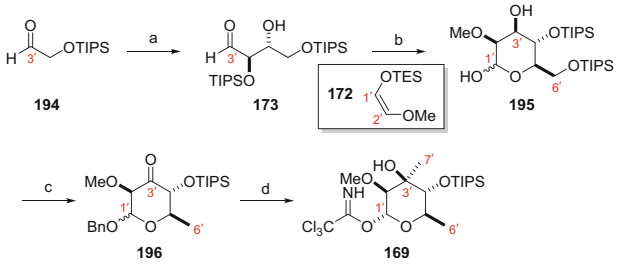

Scheme 40 Organocatalytic approach to D-configured callipeltose C. *Reagents and conditions*: (**a**) D-proline, DMF, 75%, er > 99:1; (**b**) **172**, $MgBr_2$•Et_2O, CH_2Cl_2, 47%, dr > 95:5; (**c**) (i) AcCl, BnOH, 110°C; (ii) PhOCSCl, pyridine, CH_2Cl_2; (iii) *n*-Bu_3SnH, AIBN, PhH, 120°C; (iv) Dess–Martin periodinane, CH_2Cl_2, 0°C, 47% (over 4 steps); (**d**) (i) $MgBr_2$•Et_2O, MeMgBr, CH_2Cl_2, dr > 95:5; (ii) H_2, Pd/C, EtOAc; (iii) Cl_3CCN, Cs_2CO_3, CH_2Cl_2, 86% (over 3 steps), dr = 95:5

2.8.5 Synthesis of D-Callipeltose C

The synthesis commenced with dimerisation of aldehyde **194** under organocatalytic conditions to provide **173** in good yield and excellent enantioselectivity (er > 99:1) (Scheme 40) [16, 54]. This was then subjected to the organocatalytic Mukaiyama aldol conditions developed in the MacMillan laboratory, with the Lewis acid ($MgBr_2$) and solvent (CH_2Cl_2) choice critical for the formation of the desired sugar scaffold (**195**) [16, 55, 56]. The anomeric hydroxy was then protected as its benzyl ether with concomitant removal of the primary TIPS protecting group.

Subsequent conversion of the primary alcohol to the corresponding phenyl thiocarbonate and deoxygenation under Barton–McCombie conditions provided the C6′ methyl group. Oxidation of the remaining C3′ secondary hydroxy to the ketone then gave **196**. Further manipulation by means of diastereoselective methyl Grignard addition (dr = 95:5), removal of the benzyl group and formation of the trichloroacetimidate provided the D-callipeltose C sugar coupling partner **169**. Overall, this fragment was synthesised in eight steps and 14.5% yield (Scheme 40) [16].

2.8.6 Completion of Callipeltoside C

The callipeltoside aglycon was coupled with D-callipeltose C (**169**) using the conditions developed by Tietze [16, 61] which, following TIPS deprotection, gave spectroscopic data inconsistent with the natural isolate [4]. Since previous syntheses of callipeltoside A had determined the absolute stereochemistry of the molecule, it was reasonably assumed that the problem lay with the callipeltose C sugar rather than the aglycon. As a result, the enantiomeric L-configured sugar (*ent*-**169**) was synthesised under the same conditions outlined in Scheme 40. Schmidt glycosidation and final TIPS deprotection gave compound **3**, which this time had identical spectroscopic data to naturally occurring callipeltoside C [4, 16]. This result not only confirmed the absolute stereochemistry of callipeltoside C but also suggested that both callipeltosides A and C contain L-configured sugars (Scheme 41). This was in contrast to the original structures drawn in the isolation papers [3, 4].[4] However, it is noteworthy that the glycosidic linkage attaching callipeltose C to the aglycon was only tentatively assigned, with the MacMillan group assuming it to be the β-equatorial anomer by comparison with the originally reported structure of callipeltoside B (Figs. 3, **5**) [16].

2.9 Ley Syntheses of Callipeltosides A, B and C (2012)

2.9.1 Retrosynthesis

The Ley group's approach to the entire callipeltoside family involved a highly convergent strategy whereby the molecule(s) was split into three equally sized fragments: the C1–C9 pyran (**170**), C10–C22 vinylic iodide (**197**) and the relevant sugar moiety [14, 15]. The common callipeltoside aglycon would then be assembled by union of **170** and **197** via a diastereoselective Oppolzer–Radinov alkenylzinc addition [62], followed by Yamaguchi macrolactonisation. The C1–C9 pyran was to be formed using an $AuCl_3$-catalysed cyclisation, which the group had reported

[4] An optical rotation of $[\alpha]^{25}_{D} = -23.1$ ($c = 0.18$, $CDCl_3$) was measured for synthetic callipeltoside C [16]. However, no optical rotation for natural callipeltoside C was recorded due to the prohibitively small amounts isolated [4].

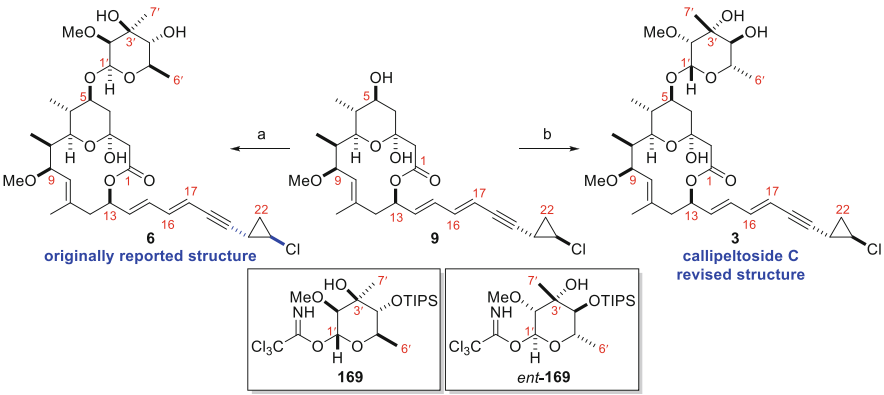

Scheme 41 Completion of callipeltoside C. *Reagents and conditions*: (**a**) (i) **169**, TMSOTf, 4 Å MS, CH_2Cl_2, −30°C; (ii) TASF, DMF, 40°C, 58% (over 2 steps); (**b**) (i) *ent*-**169**, TMSOTf, 4 Å MS, CH_2Cl_2, −30°C; (ii) TASF, DMF, 40°C, 63% (over 2 steps)

previously [63]. Since other approaches to the callipeltosides had often struggled to produce the dien-yne as a single isomer, the group also chose to address this synthetic issue. With this in mind, the C15–C16 and C17–C18 bonds were disconnected, revealing bis-stannane linchpin **201**, from which bidirectional Stille reactions could be performed. Pyranone **202** was considered to be a key building block from which each callipeltose sugar could be accessed (Scheme 42) [14, 15].

2.9.2 Synthesis of Pyran 170

Synthesis of pyran fragment **170** began with crotylation of known Roche ester-derived aldehyde **203** to give homoallylic alcohol **205** in good yield (70%) and diastereoselectivity (dr = 88:12). Conversion to the triol using catalytic osmium tetroxide followed by sodium periodate-mediated cleavage gave the requisite aldehyde, with which a chelation-controlled addition of propargyl zinc furnished diol **206** in 72% over three steps (dr = 85:15 at C5). Two further synthetic steps gave ynoate **208**, enabling all minor diastereomers to be separated (**208**, dr > 95:5) and the 1,3-*anti*-relationship to be proven by X-ray crystallography (not shown). Subsequent deprotection afforded the diol, which smoothly underwent $AuCl_3$-catalysed cyclisation in MeOH to give pyran **209** as a single, anomerically favoured diastereomer in 96% yield. Further routine synthetic manipulations gave pyran fragment **170** in 26% yield from **203** (11 linear steps) with minimal use of chromatography (Scheme 43) [14, 15].

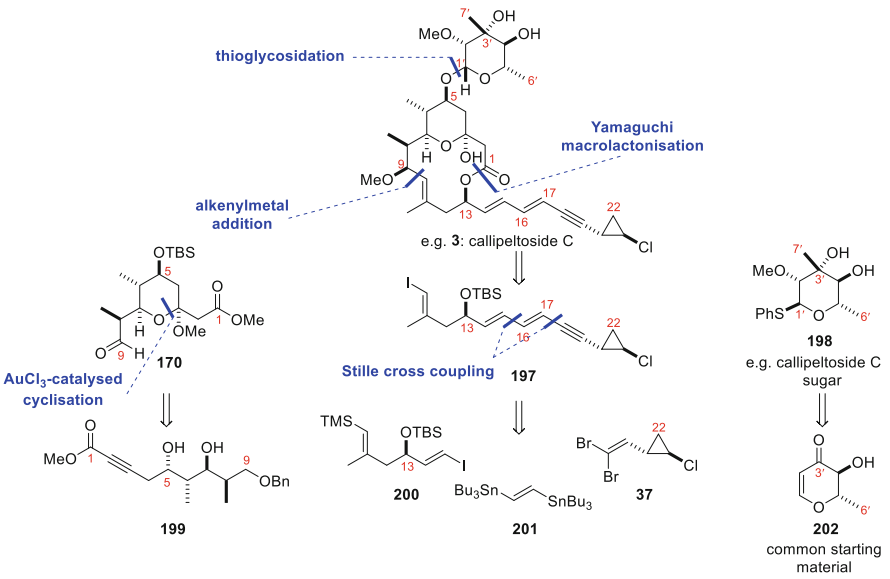

Scheme 42 Ley group approach to the callipeltosides (callipeltoside C shown for clarity)

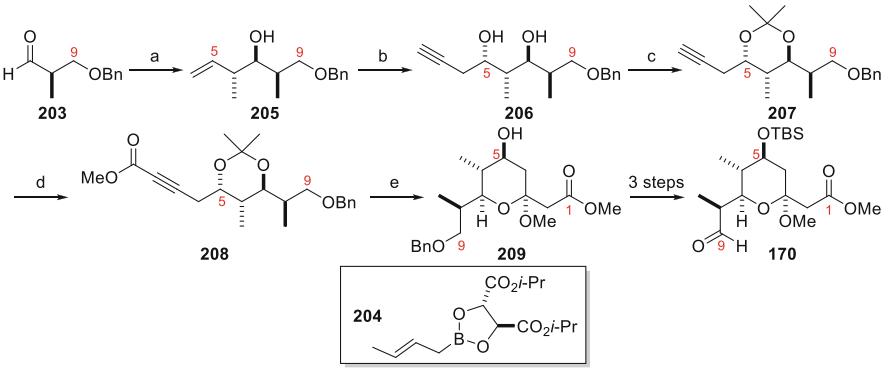

Scheme 43 Synthesis of pyran **170.** *Reagents and conditions*: (**a**) crotylborane **204**, 4 Å MS, PhMe, −78°C, 70%, dr = 88:12; (**b**) (i) OsO_4, NMO, acetone–H_2O (2:1), RT; (ii) $NaIO_4$, THF–H_2O (10:1), 0°C to RT; (iii) Zn, propargyl bromide, THF, 0°C to −100°C, 72% (over 3 steps), dr = 85:15 (at C5); (**c**) 2,2-dimethoxypropane, (±)-CSA, acetone, RT; (**d**) *n*-BuLi, THF, −40°C to −78°C, then $ClCO_2Me$, 73% (over 2 steps), dr > 95:5; (**e**) (i) QP-SA, MeOH, RT, 95%; (ii) $AuCl_3$ (2 mol%), MeOH, RT, 96%

2.9.3 Completion of the C10–C22 Fragment

In order to construct fragment **197** in a stereospecific fashion via sequential Stille cross-coupling reactions, the vinyl iodide functionality was masked in order to provide orthogonal reactivity. Work began from known vinyl iodide **210** [64, 65], which contained a vinyl silane moiety that could be converted to the corresponding vinyl iodide at a late stage. Lithiation of **210** followed by reaction with **211** gave the secondary alcohol with installation of the C13 stereocentre. A two-step protecting group manipulation provided **212** which, following oxidation, dibromoolefination and Corey–Fuchs reaction, gave alkyne **213**. Subsequent Pd-catalysed hydrostannylation and tin–iodine exchange led to the desired (*E*)-vinyl iodide **200** as a single stereoisomer [14, 15].

Stille coupling partner **215** was completed by treatment of known dibromide **37** with TBAF to give the bromoalkyne, which was then coupled to bis-stannane **201** via a low temperature (−10°C) Stille reaction with stoichiometric Ag_2CO_3 as an additive. Fragments **200** and **215** were united by a second Stille reaction to yield advanced substrate **216** which, following treatment with NIS, provided **197** in a completely stereospecific manner in good yield (Scheme 44) [14, 15].

2.9.4 Union of Fragments 170 and 197 and Macrocycle Formation

In order to couple fragments **170** and **197**, the Ley group turned to the work of Oppolzer and Radinov [62] as well as the studies of Marshall [66, 67], who had previously shown that the stereochemical information of an appropriate enantioenriched lithio *N*-methylephedrine alkoxide could be transferred to reactions of this type. The stereochemical model proposed in the literature revealed (1*R*,2*S*)-(−)-*N*-methylephedrine to be the reagent of choice; but in practice poor C9 diastereoselectivity was observed (34:66, not shown). The reaction was also performed with the enantiomeric ligand, (1*S*,2*R*)-(+)-*N*-methylephedrine, this time resulting in a much-improved C9 diastereomeric ratio of 91:9. Methylation of both diastereomeric mixtures allowed the group to intercept a known compound disclosed by MacMillan [16], meaning that the stereochemical outcome of these reactions could be straightforwardly determined. To their surprise, the diastereomerically enriched material using (1*S*,2*R*)-(+)-*N*-methylephedrine was found to be the desired compound, in contrast to the models disclosed by Oppolzer [62] and Noyori [68, 69]. It was proposed that the unexpected reversal in selectivity was due to bis-chelation between the active metal complex and the pyran oxygen, resulting in the exposure of the opposite diastereotopic face to reaction [70]. The authors note that a similar result was documented by Myers in his synthesis of the tetracycline antibiotics [70].

With the C9 stereocentre in place, the methylated derivative was deprotected and saponified to give *seco*-acid **193**. Yamaguchi macrolactonisation, and a one-pot

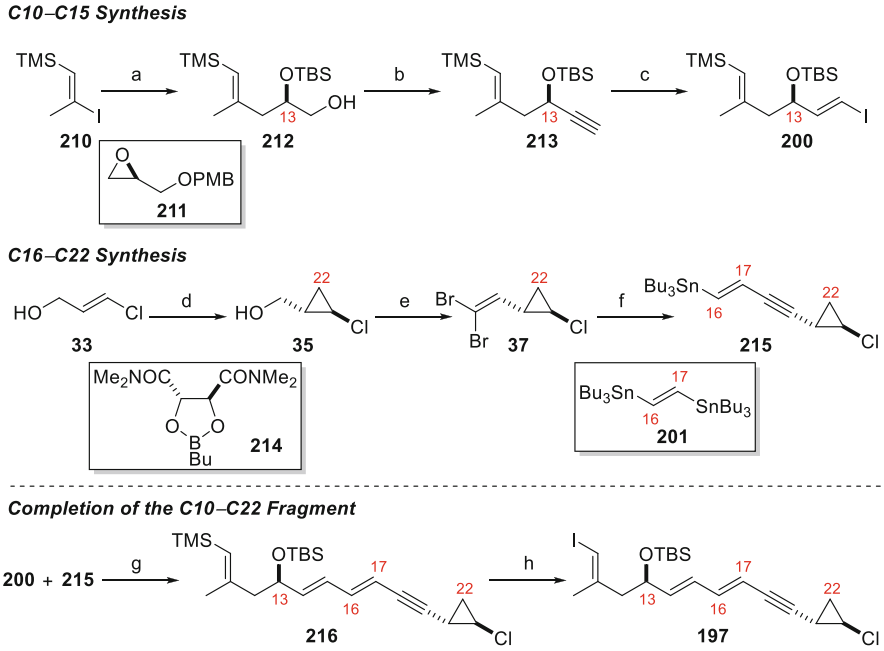

Scheme 44 Completion of the C10–C22 Fragment **197.** *Reagents and conditions*: (**a**) (i) *t*-BuLi, PhMe, −78°C, then **211**, BF_3•OEt_2, PhMe; (ii) TBSOTf, 2,6-lutidine, CH_2Cl_2, −78°C, 53% (over 2 steps); (iii) DDQ, pH 7 phosphate buffer, CH_2Cl_2, 0°C, 89%; (**b**) (i) SO_3•Py, Et_3N, DMSO, CH_2Cl_2, 0°C to RT; (ii) PPh_3, CBr_4, CH_2Cl_2, then aldehyde, 2,6-lutidine, CH_2Cl_2, 0°C, 89% (over 2 steps); (iii) *n*-BuLi, THF, −78°C, then H_2O, 85%; (**c**) (i) $Pd(PPh_3)_2Cl_2$ (3 mol%), Bu_3SnH, THF, 0°C; (ii) I_2, CH_2Cl_2, −78°C, 49% (over 2 steps); (**d**) $ZnEt_2$, CH_2I_2, CH_2Cl_2, 0°C, then **214**, **33**, CH_2Cl_2, 0°C to RT, 74%; (**e**) (i) PCC, Celite®, CH_2Cl_2, RT; (ii) PPh_3, CBr_4, CH_2Cl_2, 0°C, then aldehyde, CH_2Cl_2, 0°C to RT, 70% (over 2 steps); (**f**) (i) TBAF, DMF, 65°C; (ii) Pd_2dba_3 (10 mol%), $AsPh_3$ (40 mol%), Ag_2CO_3 (1.0 equiv.), THF, dark, −10°C, then **201**, 45% (over 2 steps); (**g**) $Pd(PFur_3)_2Cl_2$ (15 mol%), DMF, dark, RT, 63%; (**h**) NIS, MeCN, RT, 84%

deprotection/hemi-ketal formation step afforded the callipeltoside aglycon **9** (Scheme 45).

2.9.5 Preparation of Callipeltose A, B and C Thioglycosides

The synthesis of the callipeltose sugars commenced from pyranone **202**, which could be straightforwardly accessed in two steps. Nosylation of the secondary alcohol, displacement and diastereoselective methyl addition provided **218**, containing three of the stereocentres present in callipeltose A and B. Hydroxy-directed epoxidation, ring opening and selective 2° alcohol methylation gave **219**, which could be diversified to each callipeltose sugar [24]. Callipeltose A thioglycoside was completed in an additional four steps as a single anomer. Despite being able to synthesise the callipeltose B sugar, it is noted that the *N*-formyl group prevented thioglycoside

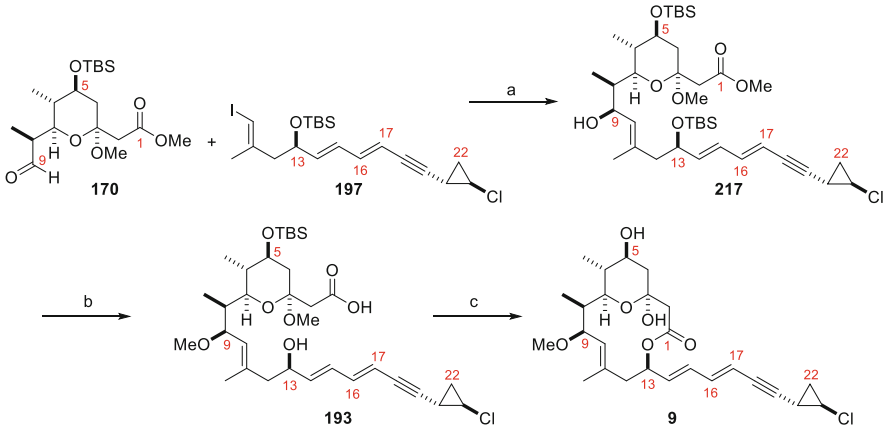

Scheme 45 Diastereoselective union of **170** and **197** and completion of the callipeltoside aglycon. *Reagents and conditions*: (**a**) 1. **197**, (1.3 equiv.), *t*-BuLi, Et_2O, −78°C; 2. $ZnBr_2$, Et_2O, −78°C to 0°C; 3. (1*S*,2*R*)-(+)-*N*-methylephedrine (1.1 equiv.), *n*-BuLi, PhMe, 0°C; 4. **170**, PhMe, 0°C, 48%; (**b**) (i) MeOTf, DTBP, CH_2Cl_2, RT, 73%; (ii) TBAF, THF, RT, 74%; (iii) $Ba(OH)_2$•$8H_2O$, MeOH, RT, quant.; (**c**) (i) 2,4,6-trichlorobenzoyl chloride, Et_3N, RT, then addition to DMAP, PhMe, 80°C; (ii) TFA, THF–H_2O (5:1), RT, 58% (over 2 steps)

formation and hence coupling to the callipeltoside aglycon. As a result, compound **219** was TMS-protected and the thioglycoside formed to give callipeltose B precursor **221**, which would have to be further manipulated once attached to the aglycon (**9**) [14, 15].

The callipeltose C sugar was also synthesised from **202**, with the C3′ stereocentre once again formed by diastereoselective methyl addition, albeit this time by means of a complex-induced proximity effect from the neighbouring C4′ hydroxy [71]. TES protection, followed by the epoxidation, ring opening, methylation and thioglycosidation sequence mentioned previously, gave the callipeltose C thioglycoside (**224**) as a single anomer (Scheme 46) [14, 15].

2.9.6 Completion of Callipeltosides A, B and C

The callipeltoside aglycon was straightforwardly coupled with thioglycoside donors **220** and **224** using the conditions described by Evans [10]. Final deprotection of these two compounds then led to callipeltosides A and C, with spectroscopic data in full agreement with that previously reported [3, 4, 14, 15].

With the syntheses of both callipeltoside A and callipeltoside C completed, attention switched to callipeltoside B. *Since there had been no previous synthesis of callipeltoside B, it was assumed that like callipeltosides A and C, it also contained an* L*-configured sugar*. Attachment of azido sugar **221** (L-configured) proceeded without incident, and the azide moiety was selectively reduced using 1,3-propanedithiol [72]. Formylation of the amine using pentafluorophenyl formate

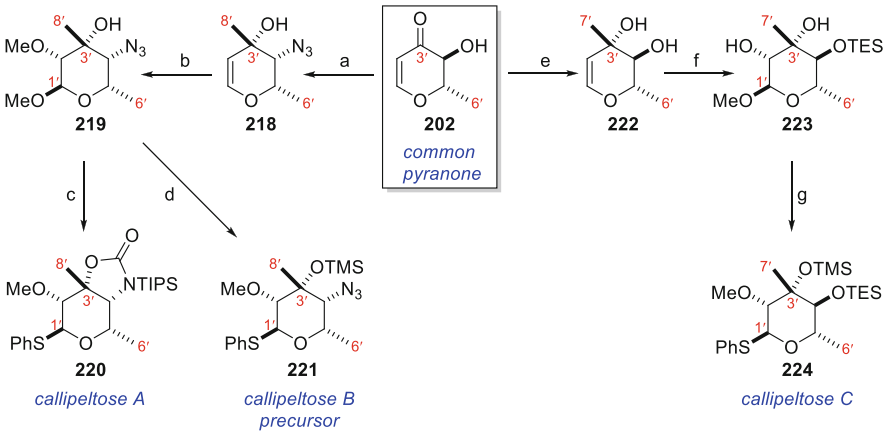

Scheme 46 Synthesis of callipeltoses A, B and C from common pyranone **202.** *Reagents and conditions*: (**a**) (i) NsCl, pyridine, CH_2Cl_2, RT, 95%; (ii) *n*-Bu_4NN_3, CH_2Cl_2, 0°C, 72%; (iii) MeLi, THF, −100°C, 79%; (**b**) (i) *m*-CPBA, MeOH, 0°C to RT, 52%; (ii) KO*t*-Bu, MeI, THF, 0°C, 79%; (**c**) (i) H_2, $Pd(OH)_2$/C, EtOAc, RT, 93%; (ii) triphosgene, pyridine, THF, −78°C to RT, 72%; (iii) TIPSOTf, 2,6-lutidine, CH_2Cl_2, RT, 97%; (iv) PhSH, BF_3•OEt_2, CH_2Cl_2, 0°C to RT, 80%, single anomer; (**d**) ZnI_2, TBAI, TMSSPh, DCE, 65°C, 60%, single anomer; (**e**) MeLi•LiBr, Et_2O, −78°C, 78%; (**f**) (i) TESCl, pyridine, DMAP, CH_2Cl_2, RT; (ii) *m*-CPBA, MeOH, 0°C to RT, 45% (over 2 steps); (**g**) (i) KO*t*-Bu, MeI, THF, 0°C, 81%; (ii) ZnI_2, TBAI, TMSSPh, DCE, 65°C, 86%, single anomer

(**225**) [73] and deprotection then delivered putative callipeltoside B (**2**) as a 4:1 rotameric mixture (by ^{1}H NMR) (Scheme 47). The synthetic sample was in complete agreement with the spectroscopic data for the natural isolate disclosed by Minale [4, 14, 15].

In order to ensure that the correct sugar had indeed been attached, the enantiomeric thioglycoside (*ent*-**221**, D-configured) was synthesised in analogous fashion to that shown in Scheme 46 and attached to the callipeltoside aglycon (**9**). This was then also reduced, formylated and deprotected to afford diastereomer **226**, which had a significantly different ^{1}H NMR to the natural isolate [4]. This provided further evidence that all three callipeltose sugars were L-configured, with callipeltoside B completed for the first time [14, 15].

With the entire family of molecules completed, the configuration of the glycosidic linkages in callipeltosides B and C still needed to be determined.

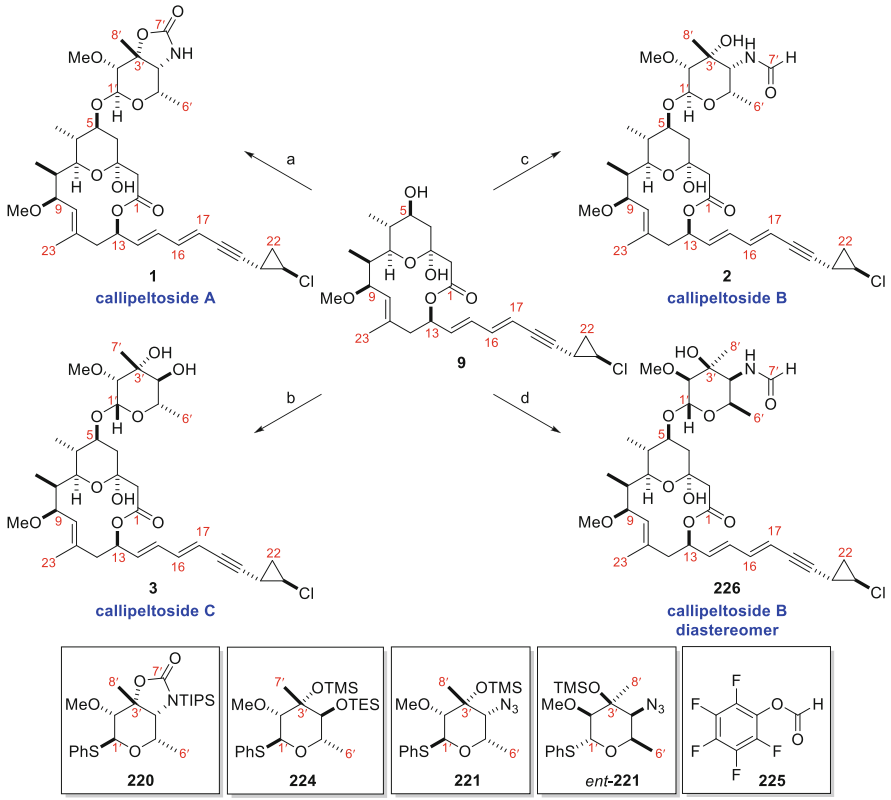

Scheme 47 Completion of callipeltosides A, B and C. *Reagents and conditions*: (**a**) (i) **220**, 4 Å MS, DTBMP, CH_2Cl_2, RT, 50 min, then −15°C, NIS, TfOH, −15°C to RT; (ii) TBAF, THF, RT, 83% (over 2 steps); (**b**) (i) **224**, 4 Å MS, DTBMP, CH_2Cl_2, RT, 50 min, then −15°C, NIS, TfOH, −15°C to RT; (ii) TASF, DMF, 40°C, 57% (over 2 steps); (**c**) (i) **221**, 4 Å MS, DTBMP, CH_2Cl_2, RT, 50 min, then −15°C, NIS, TfOH, −15°C to RT, 56%; (ii) 1,3-propandithiol, Et_3N, pyridine–H_2O (10:1), RT; (iii) **225**, $CHCl_3$, RT; (iv) TASF, DMF, 40°C, 52% (over 3 steps), 4:1 rotameric mixture (by ^1H NMR); (**d**) (i) *ent*-**221**, 4 Å MS, DTBMP, CH_2Cl_2, RT, 50 min, then −15°C, NIS, TfOH, −15°C to RT, 41%; (ii) 1,3-propandithiol, Et_3N, pyridine–H_2O (10:1), RT; (iii) **225**, $CHCl_3$, RT; (iv) TASF, DMF, 40°C, 57% (over 3 steps), 4:1 rotameric mixture (by ^1H NMR)

2.9.7 Stereochemistry of the Glycosidic Linkages of Callipeltosides B and C

Callipeltoside C

Although the Ley group had completed the second total synthesis of callipeltoside C, the configuration of the glycosidic linkage was still under question, with the MacMillan group tentatively assigning the stereochemistry by comparison with the assumed glycosidic linkage found in callipeltoside B [16]. As a result, the Ley

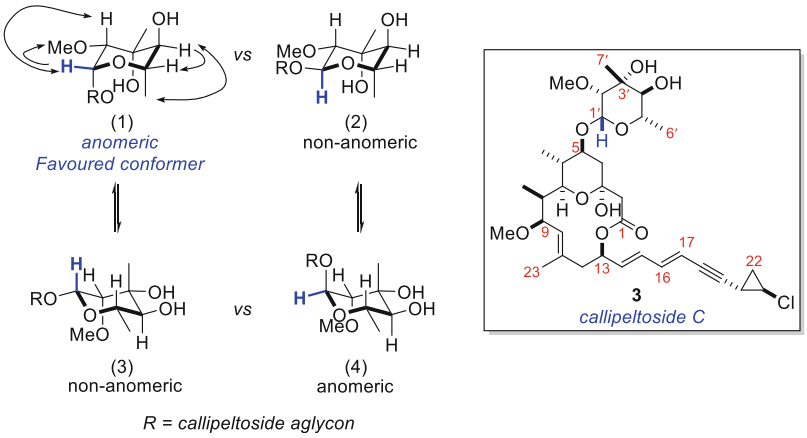

Fig. 6 Key nOe's for callipeltose C

group attempted to determine the C1′ stereochemistry by analysis of the $^{1}J_{C–H}$ coupling constant [74–78] and NOESY data.

$^{1}J_{C–H}$ *Coupling Constant*

Since measurement of the $^{1}J_{C–H}$ coupling constant [from a HSQC (heteronuclear single quantum coherence) experiment without ^{13}C decoupling] had proven to be a useful technique for carbohydrate chemists to determine whether the proton at an anomeric centre is axial or equatorial, this was assessed initially. It is noted that a value of ~170 Hz suggests an equatorial proton at C1′H, whilst ~160 Hz is indicative of an axial proton [74–78]. Unfortunately, measurement of the $^{1}J_{C–H}$ coupling constant gave an inconclusive result, returning a value of $^{1}J_{C\text{-}H} = 166.5$ Hz.

NOESY Data

As an alternative method to determine the stereochemistry of the glycosidic linkage, the Ley group conducted NOESY experiments and assessed all potential chair conformers (**1**)–(**4**) (Fig. 6; X-ray analysis of sugar intermediates suggested a chair configuration, not shown). Analysis of this averaged data indicated that structure (**1**) was the only chair conformer that accounted for all observed nOe interactions [14, 15]. With this in mind, the C1′ stereocentre was assigned to be (*R*)-configured, in agreement with the assignment previously suggested by MacMillan [16].

Callipeltoside B

The C1′H stereochemistry of callipeltoside B was analysed in exactly the same way as for callipeltoside C. Once again, the $^{1}J_{C–H}$ coupling value gave no indication of

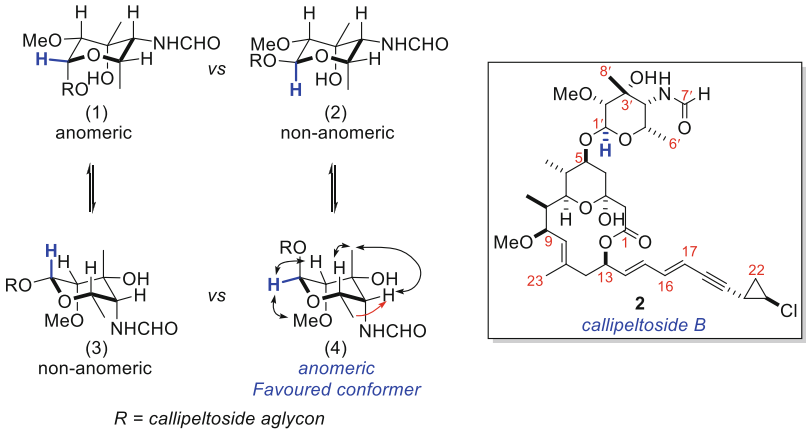

Fig. 7 Key nOe's for callipeltose B

stereochemistry, with a coupling constant of $^{1}J_{C-H} = 165.6$ Hz measured. The stereochemistry was therefore inferred from NOSEY experiments (Fig. 7). This method revealed conformer (**4**) to be the only structure accounting for all observed nOe interactions. Therefore, callipeltoside B was noted to have a (*S*)-configured glycoside linkage (Fig. 7) [14, 15].

The authors note that whilst the same glycosidic linkage is present in both callipeltosides A (**1**) and B (**2**) [(*S*)-configured], callipeltoside C (**3**) is oppositely configured [(*R*)-configured]. Since each callipeltose sugar was attached under identical glycosidation conditions, it was assumed that the stereochemical course of the reaction must be influenced by the C4′ substituent. However, at present no further work has been reported to further study this [14, 15].

3 Conclusion and Final Remarks

The completion of the callipeltosides represents nearly 20 years of synthetic work, spanning across multiple research groups. Early syntheses focused on determining the configuration of the *trans*-chlorocyclopropane ring with respect to the C1–C19 core, in the process determining the absolute stereochemistry of the callipeltoside aglycon. The synthesis of callipeltoside A was accomplished shortly thereafter. These routes evolved over time, with more elegant and convergent approaches implemented once the stereochemical ambiguities associated with the aglycon had been overcome. The final pieces of the puzzle concerned the absolute configuration of the callipeltose B and C sugars, whilst the stereochemistry of the anomeric linkage of these molecules remained uncertain. The MacMillan and Ley groups later provided evidence to suggest that all members of the family contained L-configured sugars (having both also synthesised the corresponding D-configured callipeltose B

and C sugars), with the latter research group further analysing the stereochemistry at C1′H to complete the study.

The different approaches towards the callipeltosides highlighted in this review stand as a testament to the power of modern synthetic technologies in their ability to supplement classical natural product structural analysis. It provides access to novel analogues and, in the programme above on the callipeltosides, makes available significantly greater quantities of material than that which is obtained by extraction from natural sources.

References

1. Zampella A, D'Auria MV, Paloma LG, Casapullo A, Minale L, Debitus C, Henin Y (1996) J Am Chem Soc 118:6202–6209
2. D'Auria MV, Zampella A, Paloma LG, Minale L (1996) Tetrahedron 52:9589–9596
3. Zampella A, D'Auria MV, Minale L, Debitus C, Roussakis C (1996) J Am Chem Soc 118:11085–11088
4. Zampella A, D'Auria MV, Minale L (1997) Tetrahedron 53:3243–3248
5. Yeung K, Paterson I (2005) Chem Rev 105:4237–4313
6. Paterson I, Findlay AD (2008) Pure Appl Chem 80:1773–1782
7. Trost BM, Dirat O, Gunzner JL (2002) Angew Chem Int Ed 41:841–843
8. Trost BM, Gunzner JL, Dirat O, Rhee YH (2002) J Am Chem Soc 124:10396–10415
9. Evans DA, Hu E, Burch JD, Jaeschke G (2002) J Am Chem Soc 124:5654–5655
10. Evans DA, Burch JD, Hu E, Jaeschke G (2008) Tetrahedron 64:4671–4699
11. Paterson I, Davies RDM, Heimann AC, Marquez R, Meyer A (2003) Org Lett 5:4477–4480
12. Huang H, Panek JS (2004) Org Lett 6:4383–4385
13. Hoye TR, Danielson M, May AE, Zhao H (2010) J Org Chem 75:7052–7060
14. Frost JR, Peason CM, Snaddon TN, Booth RA, Ley SV (2012) Angew Chem Int Ed 51:9366–9371
15. Frost JR, Pearson CM, Snaddon TN, Booth RA, Turner RM, Gold J, Shaw DM, Gaunt MJ, Ley SV (2015) Chem Eur J 21:13261–13277
16. Carpenter J, Northrup AB, Chung D, Wiener JJM, Kim S, MacMillan DWC (2008) Angew Chem Int Ed 47:3568–3572
17. Paterson I, Davies RDM, Marquez R (2001) Angew Chem Int Ed 40:603–607
18. Marshall JA, Eidam PM (2008) Org Lett 10:93–96
19. Velazquez F, Olivo HF (2000) Org Lett 2:1931–1933
20. Olivo HF, Velazquez F, Trevisan HC (2000) Org Lett 2:4055–4058
21. Romero-Ortega M, Colby DA, Olivo HF (2002) Tetrahedron Lett 43:6439–6441
22. Yadav JS, Haldar A, Maity T (2012) Eur J Org Chem:2062–2071
23. Gurjar MK, Reddy R (1998) Carbohydr Lett 3:169–172
24. Pihko AJ, Nicolaou KC, Koskinen AMP (2001) Tetrahedron Asymmetry 12:937–942
25. Smith GR, Finley JJ, Giuliano RM (1998) Carbohydr Res 308:223–227
26. Toth A, Remenyik J, Bajza I, Liptak A (2003) ARKIVOC:28–45
27. Saito S, Shiozawa M, Ito M, Yamamoto H (1998) J Am Chem Soc 120:813–814
28. Saito S, Shiozawa M, Yamamoto H (1999) Angew Chem Int Ed 38:1769–1771
29. Paterson I, Goodman JM, Isaka M (1989) Tetrahedron Lett 30:7121–7124
30. Paterson I, Perkins MV (1992) Tetrahedron Lett 33:801–804

31. Paterson I, Norcross RD, Ward RA, Romea P, Lister MA (1994) J Am Chem Soc 116:11287–11314
32. Charette AB, Juteau H (1994) J Am Chem Soc 116:2651–2652
33. Charette AB, Prescott S, Brochu C (1995) J Org Chem 60:1081–1083
34. Wang T, Liang Y, Yu Z (2011) J Am Chem Soc 133:9343–9353
35. Trost BM, Gunzner JL (2001) J Am Chem Soc 123:9449–9450
36. Sone H, Kigoshi H, Yamada K (1996) J Org Chem 61:8956–8960
37. Trost BM, Toste FD, Pinkerton AB (2001) Chem Rev 101:2067–2096
38. Trost BM, Toste FD (1999) J Am Chem Soc 121:4545–4554
39. Trost BM, Belletire JL, Godleski S, McDougal PG, Balkovec JM (1986) J Org Chem 51:2370–2374
40. Barton DHR, Crich D, Motherwell WB (1983) Tetrahedron Lett 24:4979–4982
41. Shen W, Wang L (1999) J Org Chem 64:8873–8879
42. Evans DA, Kozlowski MC, Murray JA, Burgey CS, Connell B (1999) J Am Chem Soc 121:669–685
43. Evans DA, Burch JD (2001) Org Lett 3:503–505
44. Masuda Y, Hoshi M, Arase A (1992) J Chem Soc Perkin Trans 1:2725–2726
45. Furukawa J, Kawabata N, Nishimura J (1968) Tetrahedron 24:53–58
46. Denmark S, O'Conner SP (1997) J Org Chem 62:3390–3401
47. Yang Z, Lorenz JC, Shi Y (1998) Tetrahedron Lett 39:8621–8624
48. Frank SA, Chen H, Kunz RK, Schnaderbeck MJ, Roush WR (2000) Org Lett 2:2691–2694
49. Evans DA, Hu E, Tedrow JS (2001) Org Lett 3:3133–3136
50. Masse CE, Panek JS (1995) Chem Rev 95:1293–1316
51. Huang HB, Panek JS (2003) Org Lett 5:1991–1993
52. Hoye TR, Zhao H (1999) Org Lett 1:169–172
53. Hoye TR, Danielson ME, May AE, Zhao H (2008) Angew Chem Int Ed 47:9743–9746
54. Northrup AB, MacMillan DWC (2002) J Am Chem Soc 124:6798–6799
55. Northrup AB, Mangion IK, Hettche F, MacMillan DWC (2004) Angew Chem Int Ed 43:2152–2154
56. Northrup AB, MacMillan DWC (2004) Science 303:1752–1755
57. Brown SP, Brochu MP, Sinz CJ, MacMillan DWC (2003) J Am Chem Soc 125:10808–10809
58. Zhong G (2003) Angew Chem Int Ed 42:4247–4250
59. Marshall JA, Yanik MM (2000) Tetrahedron Lett 41:4717–4721
60. Semmelhack MF, Kim C, Zhang N, Bodurow C, Sanner M, Dobler W, Meier M (1990) Pure Appl Chem 62:2035–2040
61. Tietze LF, Fischer R, Guder HJ, Goerlach A, Meumann M, Krach T (1987) Carbohydr Res 164:177–194
62. Oppolzer W, Radinov RN (1991) Tetrahedron Lett 32:5777–5780
63. Diéguez-Vázquez A, Tzschucke CC, Crecente-Campo J, McGrath S, Ley SV (2009) Eur J Org Chem:1698–1706
64. Nicolaou KC, Chakraborty TK, Piscopio AD, Minowa N, Bertinato P (1993) J Am Chem Soc 115:4419–4420
65. Nicolaou KC, Piscopio AD, Bertinato P, Chakraborty TK, Minowa N, Koide K (1995) Chem Eur J 1:318–333
66. Marshall JA, Eidam P (2004) Org Lett 6:445–448
67. Layton ME, Morales CA, Shair MD (2002) J Am Chem Soc 124:773–775
68. Pu L, Yu H (2001) Chem Rev 101:757–824
69. Noyori R, Suga S, Kawai K, Okada S, Kitamura M, Oguni N, Hayashi M, Kaneko T, Matsuda Y (1990) J Organomet Chem 382:19–37
70. Brubaker JD, Myers AG (2007) Org Lett 9:3523–3525
71. Beak P, Meyers AI (1986) Acc Chem Res 19:356–363
72. Bayley H, Standring DN, Knowles JR (1978) Tetrahedron Lett 19:3633–3634
73. Kisfaludy L, Ötvös L (1987) Synthesis:510

74. Muller N, Pritchard DE (1959) J Chem Phys 31:768–771
75. Maciel GE, McIver Jr JW, Ostlund NS, Pople JA (1970) J Am Chem Soc 92:1–11
76. Bock K, Lundt I, Pedersen C (1973) Tetrahedron Lett 13:1037–1040
77. Bock K, Wiebe L (1973) Acta Chem Scand 27:2676–2678
78. Bock K, Pedersen C (1974) J Chem Soc Perkin Trans 1:293–299